STUDY OF THE CONFORMATION OF MYOGLOBIN ADSORBED ON NANOPARTICLES USING HYDROGEN/DEUTERIUM EXCHANGE MASS SPECTROMETRY

By

YAOLING LONG

A THESIS PRESENTED TO THE GRADUATE SCHOOL
OF THE UNIVERSITY OF FLORIDA IN PARTIAL FULFILLMENT
OF THE REQUIREMENTS FOR THE DEGREE OF
MASTER OF SCIENCE

UNIVERSITY OF FLORIDA

2009

To my family

ACKNOWLEDGMENTS

I would like to thank my advisor, Dr. John R. Eyler, for his great support and guidance during my graduate study. Dr. Eyler taught me not only how to do scientific research, but also how to be a person that can be helpful to others and to this society. Dr. Eyler is like a great friend. I still remember the first time when he talked to me about this project. I want to thank for all his advices and help in every aspect of my life.

I would like to thank my co-advisor, Dr. David S. Barber, for his generosity offering me the opportunity to work on this project. His support, encouragement, help and suggestions have been critical in continuing my research. The travel experience to the University of South Florida with him will be good memories to me.

I would like to thank my committee member, Dr. David H. Powell, for his great suggestions and help. I have to admit that I should have cherished the time to learn more from him.

Appreciation is given to Dr. Benjamin W. Smith for his advice and guidance, and Ms. Lori Clark for her patience and support.

I want to express my gratitude to Dr. Mark Emmett at Florida State University, and Dr. Stan Stevens at the University of South Florida, for their great help offering the time and instrument on sample analysis. Dr. Jeremiah Tipton at Florida State University also provided great help and suggestions. I also want to thank Dr. Nick Polfer for his precious comments and discussions on the project and on my presentation.

I would like to thank Dr. Jodie Johnson for his great patience in teaching me the fundamental knowledge on mass spectrometry. I would like to thank Scott Wasdo for the adsorption isotherm experiment, many thanks to Roxanne Werner, John Munson, Kevin Kioll, April Feswick, Nick Doperalski in the Center for Human and Environmental

Toxicology, and other friends. Their friendship and help will be my long time treasure. I would like to thank all my group members also: Michelle, Julia, Jhoana, Sarah, Joanna, Lee, and Cesar, for their kind support during my graduate study.

Enough thanks could not be said to my husband, my son, and my parents for their moral support, guidance, encouragement, and most importantly, love.

TABLE OF CONTENTS

page

LIST OF FIGURES

LIST OF ABBREVIATIONS

A	Arrhenius coefficient
A_b	amount of protein bound to nanoparticles
A_{max}	maximum amount of protein bound to nanoparticles
B	magnetic field strength
BET	Brunauer, Emmett and Teller
Bis	bisacrylamide
c	concentration
CD	circular dichroism
COSY	correlation spectroscopy
DC	direct circuit
DSC	differential scanning calorimetry
E_a	reaction activation energy
ESI	electrospray ionization
FDA	Food and Drug Administration
FTICR	Fourier Transform Ion Cyclotron Resonance
HDEX	Hydrogen/Deuterium exchange
HEPES	N-2-hydroxyethylpiperazine-N'-2-ethanesulfonic acid
HMC	heated metal capillary
HPLC	High performance liquid chromatography
HSQC	heteronuclear single quantum coherence
ICR	ion cyclotron resonance
k	chemical reaction rate constant
k	Langmuir adsorption constant
k_1	unfolding rate constant

k_{-1}	folding rate constant
k_2	intrinsic chemical exchange rate constant
k_{ex}	hydrogen/deuterium exchange rate constant
k_{obs}	observed rate constant
LTQ	Linear Trap Quadrupole
m_1	exchange hydrogens in side chain and terminal of peptides
m_2	exchangeable hydrogens on amide bonds in peptides
MS	mass spectrometry
NHMFL	National High Magnetic Field Laboratory
NMR	nuclear magnetic resonance
NOESY	nuclear overhauser effect spectroscopy
PAGE	polyacrylamide gel electrophoresis
PBS	phosphate buffered saline
QIT	quadrupole ion trap
Q-TOF	quadrupole-time of flight
R	universal gas constant
RF	radio frequency
SDS	Sodium dodecyl sulfate
T	Tesla
t	hydrogen/deuterium exchange time
TOF	time of flight
Tris	tris(hydroxymethyl)aminomethane
Trp	Tryptophan
UV	Ultra Violet
θ	ellipticity (in degrees)

θ	percentage of deuterium atoms for all hydrogen isotope atoms
ΔM	mass increase after hydrogen/deuterium exchange

Abstract of Thesis Presented to the Graduate School
of the University of Florida in Partial Fulfillment of the
Requirements for the Degree of Master of Science

STUDY OF THE CONFORMATION OF MYOGLOBIN ADSORBED ON NANOPARTICLES USING HYDROGEN/DEUTERIUM EXCHANGE MASS SPECTROMETRY

By

Yaoling Long

December 2009

Chair: John R. Eyler
Major: Chemistry

This thesis reports the study of the conformational change of myoglobin adsorbed on nanoparticles using hydrogen/deuterium (H/D) exchange mass spectrometry. The peptide identification and sequence mapping were carried out for myoglobin in solution as well as adsorbed on silver and nickel nanoparticles. H/D exchange of myoglobin in solution was performed and the results were compared with those in literature.

Two different enzymes, pepsin and protease XIII, were evaluated as fragmentation agents prior to the mass spectrometric analysis of myoglobin. Compared to pepsin, protease XIII produces peptide fragments of myoglobin in different patterns, as well as more short residues.

Hydrogen/deuterium exchange for myoglobin on silver nanoparticles was investigated first on a 14.5 T Fourier Transform Ion Cyclotron Resonance (FTICR) mass spectrometer and then on a Linear Trap Quadrupole (LTQ)-Orbitrap mass spectrometer. When preparing samples for the 14.5 T FTICR, contamination was observed. The sources of contamination were identified using the gel electrophoresis technique. Preliminary H/D exchange mass spectrometry experiments for myoglobin on

nanoparticles were performed later using the LTQ-Orbitrap mass spectrometer. The mass increases of peptide residues for myoglobin adsorbed on silver nanoparticles were significantly greater than those observed when myoglobin is in solution. The preliminary results indicate that the method development reported in this thesis is very promising for the investigation of protein conformational changes on nanoparticles.

CHAPTER 1
INTRODUCTION

Background

Nanoparticles, particles 100 nm or less in size in at least one dimension, such as metals (gold, silver), metal oxides (TiO_2, SiO_2), inorganic materials (carbon nanotubes, quantum dots), and polymeric materials, have received considerable attention recently in both diagnostics and therapeutics, primarily due to their potential benefits in the specificity of targeted drug delivery[1, 2]. Nanoparticles have also found wide application in many other fields, including cosmetics, electronics, and the automotive industry. Under those manufacturing circumstances, it is not surprising that nanoparticles may enter into the bodies of workers who are in close contact with them, by inhalation, dermal contact or ingestion. For both of these reasons, the toxicological impacts of nanoparticles on human health are of concern[3]. However, currently there is no clear understanding of the mechanisms of nanoparticle behavior in the human body.

Nanoparticles' primary action in human body may be initiated by the adsorption of certain serum proteins on the particles' surfaces[4, 5]. As a general rule, when exposed to proteinaceous environments, such as plasma, nanoparticles are coated with proteins immediately. Protein adsorption on nanoparticles' surfaces may result in surface exposure of residues (cryptic epitopes) that are normally hidden in the protein core[6]. The unfolding of cryptic epitopes could trigger inappropriate cellular processes, but the protein structure after exposure of these residues is still similar enough to that of the native protein so that the cells can not recognize the difference. Even after desorption from the nanoparticle surface, some of these conformational changes are irreversible[7, 8]. For either of the above cases, a clear understanding of the interactions between

nanomaterials and proteins in physiological systems is critical for the development of new and more appropriate nanomaterials and for evaluation of their toxicity. In particular, a complete understanding of these kinds of interactions may help prevent adverse response in the immune system[6, 9] when nanomaterials are used in therapy.

Various methods have been used to study the conformational changes of proteins adsorbed on nanoparticles. These methods include molecular light fluorescence, differential scanning calorimetry (DSC), and circular dichroism (CD)[10, 11]. Although some of these methods are very sensitive to the protein conformational changes, they have their disadvantages, such as inability to detect 3-dimensional structural changes, susceptibility to interferences, and problems in monitoring residue-specific information.

The hydrogen/deuterium exchange technique has been widely used in exploring protein conformation for the past 30 years. Usually H/D exchange is combined with nuclear magnetic resonance (NMR) spectroscopy[12, 13]. By observing the chemical shifts of specific hydrogens, information at many sites of the protein can be obtained. However, NMR usually requires concentrations as high as the mM level, which are often not feasible for many proteins due to aggregation at these concentrations. It is also difficult to use NMR to study proteins with very high molecular weights[14].

Recently, mass spectrometry (MS) combined with H/D exchange (HDEX) has been used to explore protein conformation. The benefits of using mass spectrometry include: (1) low detection limits; (2) the capability to analyze very large proteins; and (3) the possibility of obtaining local charge information for peptides when using the electrospray ionization (ESI) technique. Usually, the resolution is at the level of 5-10 residues, making HDEX-MS a medium resolution technique. However, the resolution

may be improved by using various proteases to produce different fragments for the same protein.

Motivation

Buijs et al.[15] used H/D exchange FTICR-MS to study the conformation and dynamics of myoglobin adsorbed on silica nanoparticles. Their results showed that HDEX-MS can be used to detect local conformational changes and dynamics associated with protein adsorption on nanoparticles. Many types of materials can be used for nanoparticle synthesis, including polymers, metals, and metal oxides[6]. Protein adsorption behavior may be affected by a variety of nanoparticle properties, including shape, size, surface charge and surface composition[6, 16]. One goal of this research was to investigate the conformational changes of proteins, specifically myoglobin, adsorbed on various nanoparticles.

One issue identified in Buijs' study was the sizes of the peptide fragments, which were too large to achieve an adequate residue resolution. Buijs et al. used pepsin to partially digest the protein, but it was not possible to obtain small fragments under their experimental conditions, such as limited digestion time. Cravello et al.[17] found that a different enzyme, protease type XIII, when combined with other enzymes, can give more detailed protein structural information as well as better peptide coverage. A significant benefit is that protease type XIII is able to hydrolyze proteins to produce more fragments than pepsin or trypsin[17]. In addition, protease type XIII exhibits much less self-digestion than pepsin[18]. Another objective of this research was to use protease type XIII to study the conformational changes of myoglobin on nanoparticles by using HDEX-MS.

Objectives and Approaches

The overall objective of this research was to investigate the conformational changes of myoglobin adsorbed on nanoparticles using HDEX-MS. There were two main objectives.

The first objective was to investigate H/D exchange of myoglobin in solution. After repeating the work referenced in literature, binding isotherms of myoglobin on various nanoparticles were obtained. Silver and nickel nanoparticles were selected as the adsorption substrates. Mass spectrometry was performed for myoglobin in solution and on nanoparticles after protease digestion using protease type XIII and pepsin.

The second objective was to investigate H/D exchange of myoglobin adsorbed on nanoparticles using mass spectrometric methods. Samples were prepared and subjected to mass spectrometric analysis. Reasons for possible contamination were also explored.

Outline of the Thesis

This thesis consists of 5 chapters. This chapter has introduced background, motivation, and the objectives and approaches of the research. The second chapter reviews the literature related to the current research. The third chapter presents mass spectrometric data on myoglobin in solution and on nanoparticles before H/D exchange, as well as H/D exchange results in solution. The fourth chapter discusses the source of contamination in the samples and presents H/D exchange data for myoglobin adsorbed on silver nanoparticles. The fifth chapter is the conclusion, including suggestions for future work.

CHAPTER 2
LITERATURE REVIEW

Nanoparticles encompass particles with sizes ranging from 1 nanometer up to a hundred nanometers. In general, a decrease in particle size results in changes to physicochemical properties, for example, changes in morphology, electronic and atomic structure, phase transformation[1]. Due to the unique properties of nanoparticles, they have been used extensively in various applications, including medical diagnosis and therapy development[2, 9, 19, 20].

Nanotechnology has been listed in the FDA's "Critical Path Opportunities Report and List", which was created to provide a platform for collaborative work on critical scientific issues in medical product development and patient care[21]. Specifically, nanoparticles can act as carriers or deliverers for therapeutic drugs to reach certain targeted organs (cells) in the human body. Various types of nanoparticles have been investigated as drug carriers in treating tumors[19], such as ovarian cancer[22] and liver cancer[9].

Nanoparticles have already found wide application in many other fields, including the cosmetics, electronics, and automotive industries. Humans may be exposed to nanoparticles through inhalation, dermal contact, or ingestion. Some of these nanomaterials have been shown to be toxic[23]. However, the impacts on human health by such exposure are still not fully understood[3]. The properties of nanoparticles, such as size, shape, composition, surface area, surface charge etc, may be of importance in understanding possible toxic effects.

It is generally agreed that proteins will adsorb onto the surfaces of nanoparticles as soon as the particles enter biological fluids[4]. Upon adsorption onto the nanoparticle

surface, protein conformational changes may occur[10, 24, 25]. Different from those of “flat” surfaces, the greater curvature of the smaller nanoparticles may cause greater disruption to protein conformation[6]. Some of these changes may be irreversible[7, 8], resulting in alterations in the normal function of proteins. Research focusing on conformational changes in protein adsorbed on nanoparticles is necessary for the understanding of potential toxicological impacts of nanoparticles within the human body.

Protein Structures

Protein structure can be classified into 4 levels. The primary structure refers to the amino acid sequence of the peptide chains of a protein molecule. It is unique to a specific protein. Primary structure sometimes is called “covalent structure”, since all of the covalent bonds in protein are included in primary structure, except for disulfide bonds. The secondary structure usually refers to the regular local geometry of the main peptide chains in the protein. Alpha-helix and beta-sheet are common secondary structures. The formation of the secondary structure is mainly controlled by hydrogen bonding within the peptide backbone. As compared with the secondary structure, the tertiary structure pertains to the global, 3-dimensional geometry showing how a peptide chain folds in such a way that hydrophobic amino acid residues are hidden or “buried” within the structure, whereas hydrophilic residues are exposed on the outer surface. The formation of tertiary structure is controlled by non-covalent interactions, including hydrogen bonding, van der Waals forces, and ionic interactions. Beside the primary structure of amino acid sequences, the tertiary structure usually determines the biological activity of a protein. Conformational study of proteins usually refers to the study of secondary and tertiary structures. The quaternary structure is the stable association of 2 or more polypeptide chains, where individual chains are called

subunits. Quaternary structure is normally stabilized by non-covalent interactions, including hydrogen bonding, van der Waals forces, and ionic bonding, between subunits. Not all proteins have quaternary structure.

Studies of Protein Conformation

Methodology

Various methods have been employed to study protein conformations. However, none of the methods is perfect for all purposes. Every method has its advantages and disadvantages.

Circular dichroism

Circular dichroism (CD) spectroscopy is one of the most commonly used methods for studying protein conformation. Plane-polarized light can be considered as the resultant of 2 circularly polarized components rotating in opposite directions. These 2 components can be absorbed to different extents if the molecule is chiral, which is the case for protein molecules. Under such conditions, the transmitted light is said to have elliptical polarization represented by the ellipticity (θ) in degrees. The differential absorption of the polarized incident light can be used as a probe for showing different folding or unfolding patterns of protein molecules. Figure 2-1[26] shows far-UV CD spectra for various types of protein secondary structure. Circular dichroism can give information about secondary structure (far-UV CD), such as alpha-helix and beta-sheet formation, as well as a fingerprint of the tertiary structure (near-UV CD). However, when studying proteins adsorbed on nanoparticles, data must be interpreted with caution, because CD is very sensitive to interferences from solid particles, which can scatter the incident light. Experience in operating the instrument is also necessary to obtain satisfactory results.

Fluorescence

Fluorescence is another popular spectroscopic technique for the study of protein conformations[5, 11, 27]. Tryptophan (Trp), an aromatic amino acid residue that occurs in most proteins, fluoresces when excited with the appropriate wavelength of UV light. The fluorescence of Trp is highly sensitive to the surrounding environment. For a protein in its native state, Trp is often hidden in the hydrophobic core. When the protein unfolds, Trp may be exposed to a more hydrophilic environment, resulting in a red shift (shift to longer wavelengths) of the fluorescence due to the increased dielectric constant of the surrounding medium. Based on this principle, theoretically Trp fluorescence can be used to monitor the conformational changes of proteins, even at atomic resolution[27]. However, in practice, many factors can affect fluorescence signatures of proteins, and it is usually difficult to obtain a detailed structural interpretation.

Differential scanning calorimetry

Spectroscopic methods, such as CD, fluorescence, or infrared, often suffer from interferences due to light scattering. A non-spectroscopic method, differential scanning calorimetry (DSC) is often used as a complementary method[5, 28-31]. The principle of DSC is based on the changes of heat capacity resulting from protein conformational changes. In practice, DSC measures heat capacity of the sample as a function of temperature. Therefore, DSC can directly obtain thermodynamic data about protein conformation and stability. However, compared to the spectroscopic methods, DSC gives a general overall measure of the protein's energetics. It cannot give site specific information related to location and the nature of structural changes.

Hydrogen/Deuterium exchange

The technique of amide hydrogen/deuterium (H/D) exchange has been a powerful and popular tool in studying protein structure and dynamics since the early work by Berger and Linderstrom (1957). Labile hydrogen atoms, which include amide hydrogens, can undergo isotopic exchange with a deuterated solvent (usually deuterated water). This process can be monitored using various instrumental techniques including nuclear magnetic resonance (NMR), and more recently, mass spectrometry (MS). In protein molecules, several types of hydrogens can possibly undergo exchange: polar side-chain hydrogens attached to heteroatoms (N, O, and S), hydrogens at both the N- and C- termini, and peptide backbone amide hydrogens. However, the exchange rates vary significantly. Side-chain and terminal hydrogens usually exchange at rates much faster than those of amide hydrogens at normal physiological conditions[32, 33] and it's often beyond the capability of current detection techniques to detect these side-chain and terminal hydrogens. Thus, conventionally H/D exchange in proteins refers specifically to amide H/D exchange. Fortunately, protein conformational stability and secondary structure have significant effects on the amide hydrogens which are involved in hydrogen bonds as part of protein secondary structure and protein folding. The exchange rate for a specific amide hydrogen can provide detailed structural and stability information on that specific peptide.

H/D exchange mechanisms

As early as the 1950's, H/D exchange was used to study protein structure and conformational stability[34, 35]. H/D exchange can result from small local structural fluctuations or solvent penetration, reversible local unfolding or global unfolding reactions. Figure 2-2 gives pictorial representations for two proposed mechanisms for

H/D exchange. In the dual-pathway model[32], protein molecules undergo H/D exchange directly from the folded state. Amide hydrogens at or near the surface of the protein are assumed to exchange by this pathway via small local transient openings. These hydrogens usually do not involve any hydrogen bonding or protection from solvents. H/D exchange mediated by reversible local fluctuations or unfolding and /or global unfolding is more often described by a second pathway[32, 33]. In this mechanism, the folded protein molecule undergoes unfolding initially, either locally (as in (A)) or globally (as in (B)), followed by H/D exchange with the surrounding solvent, and completes the exchange process after re-folding. The second pathway (so-called "Linderstrom-Lang model") can be further classified into 2 types: EX1 and EX2. Generally, in either EX1 or EX2, the overall observed rate constant for H/D exchange k_{obs} can be written as[12]:

$$k_{obs} = \frac{k_1 k_2}{k_{-1}+k_2} \quad (2\text{-}1)$$

Where k_1, k_2 and k_{-1} are defined in Figure 2-2.

EX1 mechanism: The EX1 mechanism predominates when the chemical intrinsic exchange rate constant (k_2) is much faster than the refolding rate constant (k_{-1}). The observed exchange rate constant (k_{obs}) will be directly proportional to and limited by the unfolding rate constant (k_1):

$$k_{obs} = k_1 \quad (2\text{-}2)$$

This occurs when the inter-conversion of the folded and unfolded conformations is very slow, such as in the condition when a denaturant is added, or when the reaction conditions (pH, temperature, etc) change.

The intrinsic chemical rate of H/D exchange on amide hydrogens is greatly affected by pH, temperature, and solution composition. The amide H/D exchange

reaction can be catalyzed by both acid and base. The exchange has the slowest rate around pH 2-3 (Figure 2-3). According to the Arrhenius equation, the rate constant, $k = Ae^{-E_a/RT}$, is also affected by temperature *T*. Based on the activation energies (E_a) found in Bai's study[36], the exchange rate decreases 3-fold with every 10K decrease in temperature. The exchange rate can be reduced by up to 5 orders of magnitude by changing the pH from 7 at 25℃ to 2.5 at 0 ℃. This large difference in the exchange rate at different pH's and temperatures is the basis of the experimental procedure in H/D exchange study using mass spectrometry, which will be introduced later.

EX2 mechanism: When the rate constant for refolding is much greater than the intrinsic chemical exchange rate constant, the observed rate can be simplified to:

$$k_{obs} = \frac{k_1}{k_{-1}} k_2 \tag{2-3}$$

Under this condition (called the EX2 mechanism), the observed exchange rate depends on the equilibrium of the locally folding and unfolding states. If all the amide hydrogens have the same stability, i.e., the protein structure is uniformly stable along the peptide chain, H/D exchange would not provide much information about the protein stability, since there would be no difference in terms of the H/D exchange rates. Fortunately, protein local stability varies significantly and there are always some regions that are less stable than other regions. The local stability can also be changed by changing conditions. The less stable regions will have faster exchange rates. It is possible to obtain structural and conformational stability information using the H/D exchange technique. The EX2 mechanism is mostly observed under usual physiological conditions. Switching from EX2 to EX1 may occur when reaction conditions, such as pH, change significantly, to favor the intrinsic chemical reaction rate of the exchange.

Nuclear magnetic resonance spectroscopy

Combined with H/D exchange, NMR has been widely used in protein conformational studies[37]. The basic principle is that different hydrogen atoms (^{1}H, spin of ½) have different chemical shifts, while deuterium atoms (^{2}H, spin of 1) are not detected at the frequencies used to observe ^{1}H. Before performing H/D exchange, the chemical shift assignments of specific amide hydrogens are determined according to prescribed strategies[38]. Then D_2O is added, and the hydrogens are allowed to exchange. By analyzing the disappearance and the change in peak intensity or area of amide hydrogen resonances in the ^{1}H NMR after H/D exchange, information about specific amide hydrogens' stability and structure can be obtained. NMR can be used to study thermodynamic properties[39], folding intermediates[40], and conformational dynamics[12] in proteins.

With the development of NMR technology, several NMR methods can be used to monitor amide hydrogen exchange in proteins[12]. One-dimensional ^{1}H NMR is reasonably easy to understand and perform. However, multi-dimensional NMR techniques, such as correlation spectroscopy (COSY), nuclear Overhauser effect spectroscopy (NOESY) and heteronuclear single quantum coherence (HSQC), are more useful in determining the properties of site-specific amide hydrogens. The main benefit of multi-dimensional NMR spectroscopy is the correlation of hydrogens with other atoms in close proximity. For example, in ^{1}H-^{1}H COSY, amide hydrogens can be correlated with hydrogens on their alpha-carbons. In ^{15}N-HSQC, amide hydrogens are correlated with attached nitrogen atoms in ^{15}N-labeled proteins. Spectral assignment can be greatly simplified by using multi-dimensional NMR, which shows how atoms are correlated through bonds or through space. Figure 2-4[41] shows a comparison of ^{15}N-

HSQC spectra of DnaK (a protein with 638 amino acids and molecular weight of 70 kDa) in D_2O at time 0 and 24 hours. After 24 hours of exchange, some signals have disappeared, indicating that the hydrogens bonded to those nitrogens have been exchanged.

One disadvantage of NMR is that it usually requires high concentrations (normally at the mM level) of protein for the analysis, which is often impractical for many proteins with high agglomeration tendency. Another disadvantage is that NMR does not provide high resolution and accuracy for proteins larger than 30 kDa, due to resonance overlap and peak broadening.

Mass Spectrometric Methods

Since the 1990's, mass spectrometric methods used in conjunction with H/D exchange (HDEX-MS) have gained more and more popularity in protein conformational studies. Compared to the traditional NMR methods, MS methods are not site-specific, i.e., they cannot study the H/D exchange on individual amino acid residues. However, MS methods provide much better sensitivity and require much lower protein concentration (μmol to sub-μmol). MS methods can also analyze large proteins with molecular weights greater than 10^6 Da.

General Procedures

The underlying principle of HDEX-MS is the increase in mass that occurs when ^2H exchanges for ^1H. By analyzing the amount of deuterium uptake in protein molecules or peptide fragments, information on protein conformational stability and exchange dynamics can be obtained. In experimental terms, a general procedure for protein HDEX-MS is shown in Figure 2-5 and can be listed as follows:

- A concentrated protein solution is made with protic water.

- A portion of concentrated protein solution is diluted in deuterated water. The dilution ratio is usually at least 1:10 H_2O:D_2O.
- The diluted solution is incubated for certain amount of time depending on the desired extent of H/D exchange.
- An aliquot of the solution is removed and cold acid is added to decrease the pH to ~2 – 2.5, with the temperature kept at 0 ℃ to quench the exchange reaction.
- An enzymatic protease solution is added to the quenched solution to digest the protein into peptide fragments.
- The digested solution is injected into a reversed phase HPLC column and the peptides are separated.
- The peptides are analyzed by a mass spectrometer.

In HDEX-MS, electrospray ionization (ESI)[42] is the usual method of introducing charged samples into the mass spectrometer due to the ability to obtain charged intact peptides, thus greatly simplifying the spectrum and the identification process. In this sense, ESI is considered a soft ionization method. Another feature of ESI is that several H^{+1}s can be added during the ESI process, which means that the same molecule can have multiple peaks at different m/z values. By analyzing the charge-state distribution, the presence of a certain analyte can be confirmed. Additionally, electrospray ionizes molecules with almost no mass limitation. Even with very large molecules, the ability to produce multiply-charged ions greatly reduces the m/z value to a range which can be handled by mass analyzers.

Instrument

The most common mass analyzers used in protein conformation include time-of-flight (TOF), Fourier transform ion cyclotron resonance (FTICR), and most recently, Orbitrap mass spectrometers.

The principle of TOF-MS is simple. Ions with different mass/charge ratios are accelerated to the same kinetic energy by a certain potential. These ions are then introduced into a field-free tube, along which the ions drift toward the detector at different velocities depending on their masses. The travel time is proportional to the square root of the m/z value. Measuring the ion signal intensity as a function of time will produce the mass spectrum.

In an FTICR spectrometer, ions are trapped in a limited volume (cell) by applying electrostatic and magnetic fields. The Lorentz force induces the ions to move in circular cyclotron paths in the electrostatic field and the magnetic field. The frequency of this cyclotron motion is uniquely dependent on the magnetic field strength, B, and the m/z of the ion. The cyclotron motion in the cell produces an image current which oscillates at a frequency identical to that of the ions. Measurement of the image current can be used to deduce the mass spectrum after Fourier transformation of the raw data acquired in the time domain[43].

An Orbitrap is also an ion trap, similar to a quadrupole ion trap (QIT) or ICR ion trap, with neither a magnetic field nor a radio frequency (RF) oscillating electric field applied to the ions[44, 45]. Conceptually, an Orbitrap consists of a spindle-like central electrode and a barrel-like outer electrode. A DC voltage is applied between the two electrodes. Ions that are injected into the trap will have frequencies along 3 directions under the electric field: frequency of ion rotation around the central electrode, frequency of radial oscillation and frequency of axial oscillation along the central electrode. Among the 3 frequencies, only the frequency of axial oscillation is independent of an ion's properties, such as kinetic energy, injection angle, etc. This frequency is inversely

proportional to the square root of m/z value of the ions and is used for mass analysis. The axial oscillation induces an image current on the outer electrode. After Fourier transformation, the measurement of this image current can be used to obtain the mass spectrum.

Among these mass analysis techniques, FTICR has the best mass accuracy and resolution, but its instrumentation is also the most expensive and requires regular maintenance. The Orbitrap has similar mass accuracy and resolution to those of FTICR instruments, but it does not need a super-conducting magnet and is more compact and less costly.

Study of Protein Conformation on Nanoparticles

As discussed previously, adsorption of proteins on the nanoparticle surface leads to conformational changes, which possibly will cause a significant impact on protein activity, as well as the protein's interaction with other proteins (protein-protein interaction). Partial unfolding of protein may provoke adverse effects, such as over expression of inflammatory factors (for example, cytokines[46]) or reactive oxygen species[47]. Due to this, it is of critical importance to investigate the conformational changes of proteins adsorbed on nanoparticles. There have been a fair number of publications[5, 25, 29, 31] studying the conformational stability and dynamics of proteins adsorbed on nanoparticles using methods such as CD, fluorescence, and NMR. These methods have proven useful, but with the limitations described above. Although mass spectrometric methods can overcome those limitations, such studies have been rare. Buijs et at.[15] investigated the conformational stability of various local regions of myoglobin adsorbed on silica nanoparticles using H/D exchange coupled with FTICR MS. Myoglobin is a single-chain protein with 153 amino acid residues. It usually has an

iron-containing heme group in the center, around which apomyoglobin folds. Myoglobin is a common model protein which has been extensively studied for many years. Much information has been obtained about myoglobin that could be very helpful for this research. Two peptide fragments (residue 30-69 and residue 70-106), which are located in the middle of the protein chain and close the heme group, did not show stability changes after adsorption onto a nanoparticle[15]. The two terminal fragments (residue 1-29 and residue 107-137), however, were destabilized upon adsorption.

Two major issues deserve further investigation. First, the residue resolution in the Buijs et al. study was not high. The peptide fragments were too large to obtain any further local specific information. It would be desirable to produce smaller peptide fragments during digestion. Second, different substrates and proteins should be used to extend the scope of the research.

This thesis attempts to address these two issues. Two enzymatic proteases, pepsin and type XIII, were employed during the digestion and compared in terms of their fragmentation efficiencies and styles. Several metal-based nanoparticles were explored as the adsorption substrate. Silver nanoparticles were selected for most of the study.

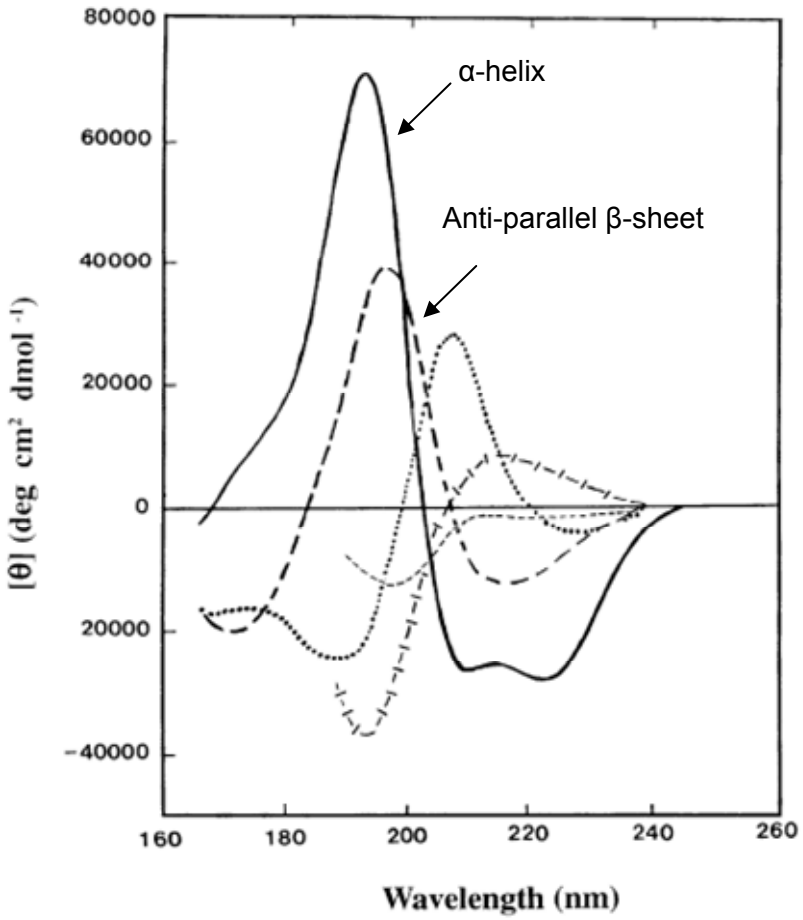

Figure 2-1. Far UV CD spectra of proteins with different structures. Solid line, a-helix; long dashed line, anti-parallel β-sheet; dotted line, type I β-turn; cross dashed line, extended 3_1-helix or poly (Pro) II helix; short dashed line, irregular structure. The figure is used with permission of Elsevier B. V.

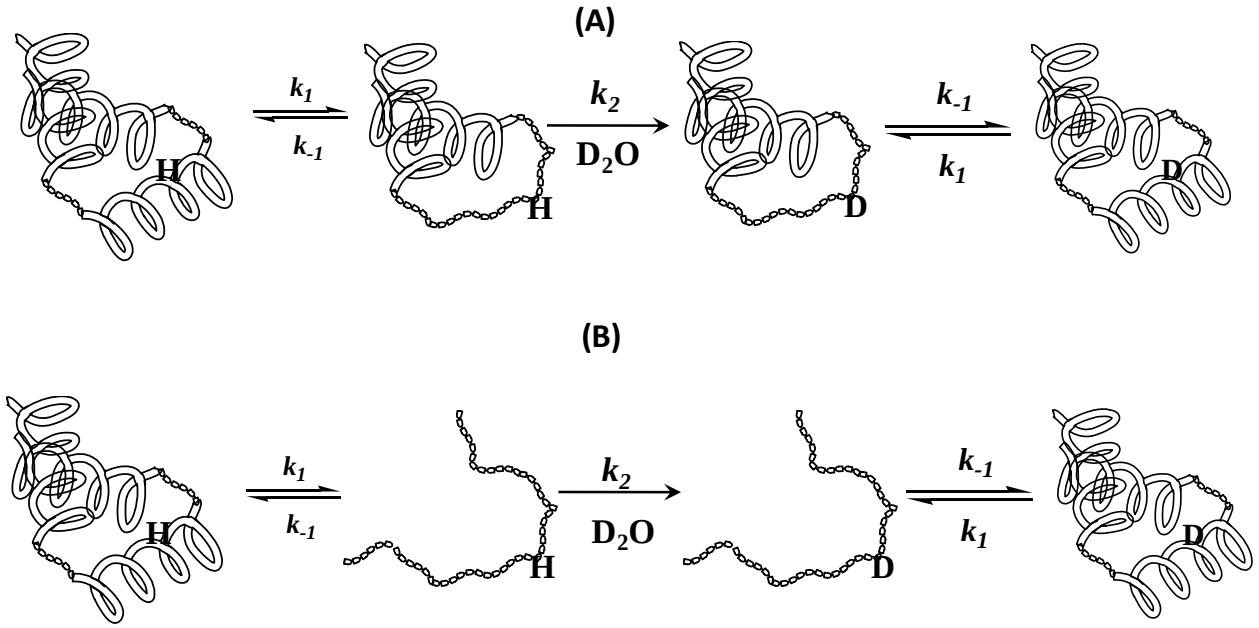

Figure 2-2. Protein H/D exchange mechanisms via local unfolding (A) or global unfolding (B)

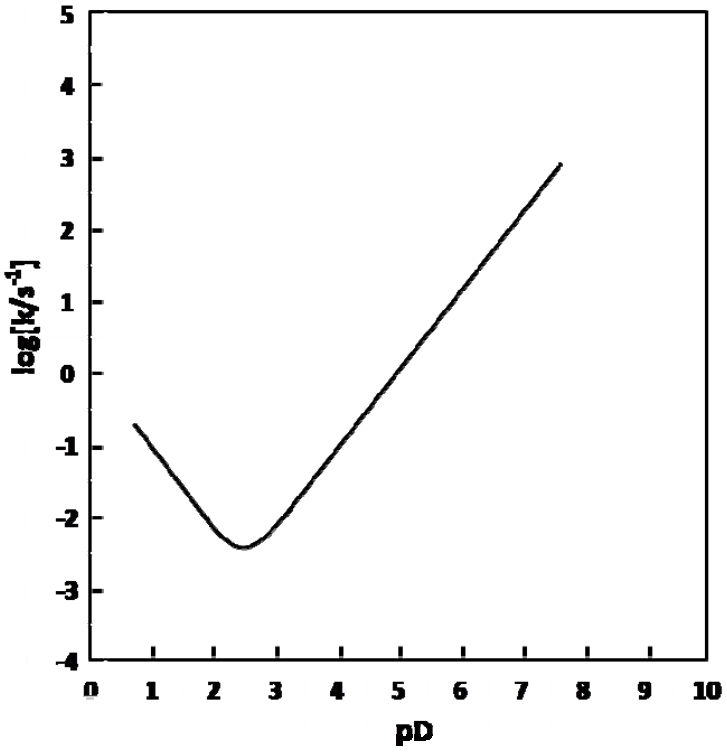

Figure 2-3. Intrinsic chemical H/D exchange rate as a function of pH

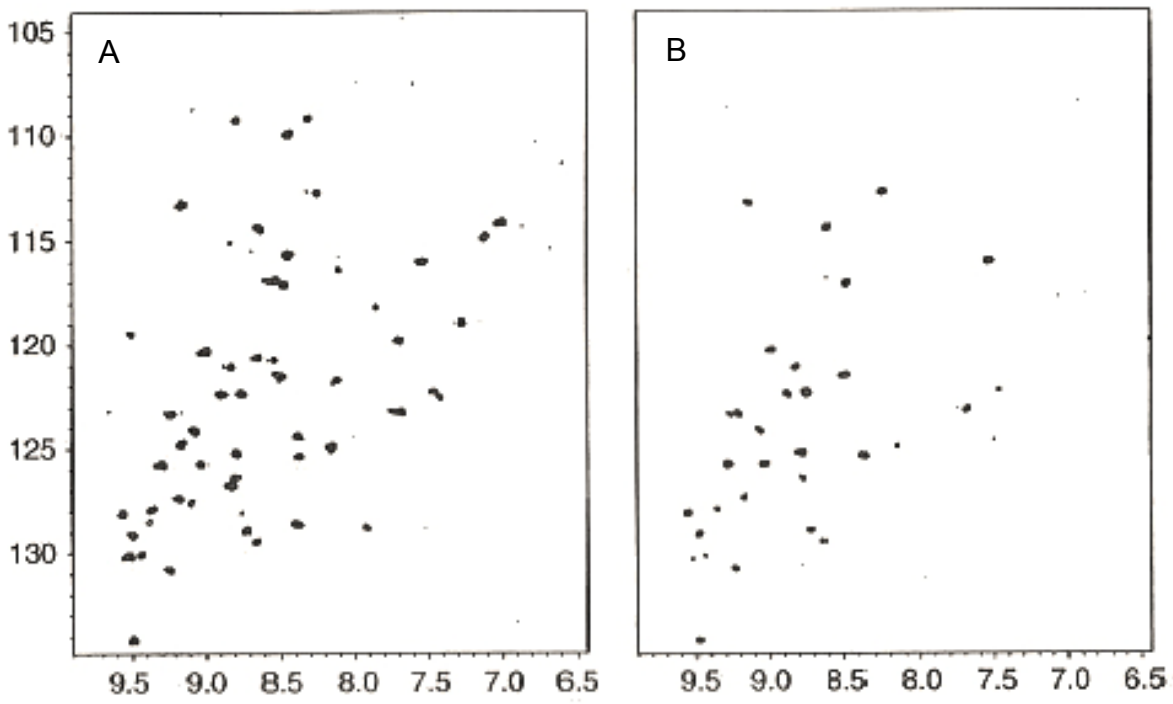

Figure 2-4. 15N-HSQC NMR spectra of DnaK before and after H/D exchange. (A) Before H/D exchange; (B) After H/D exchange. The figure is used with permission of John Wiley & Sons.

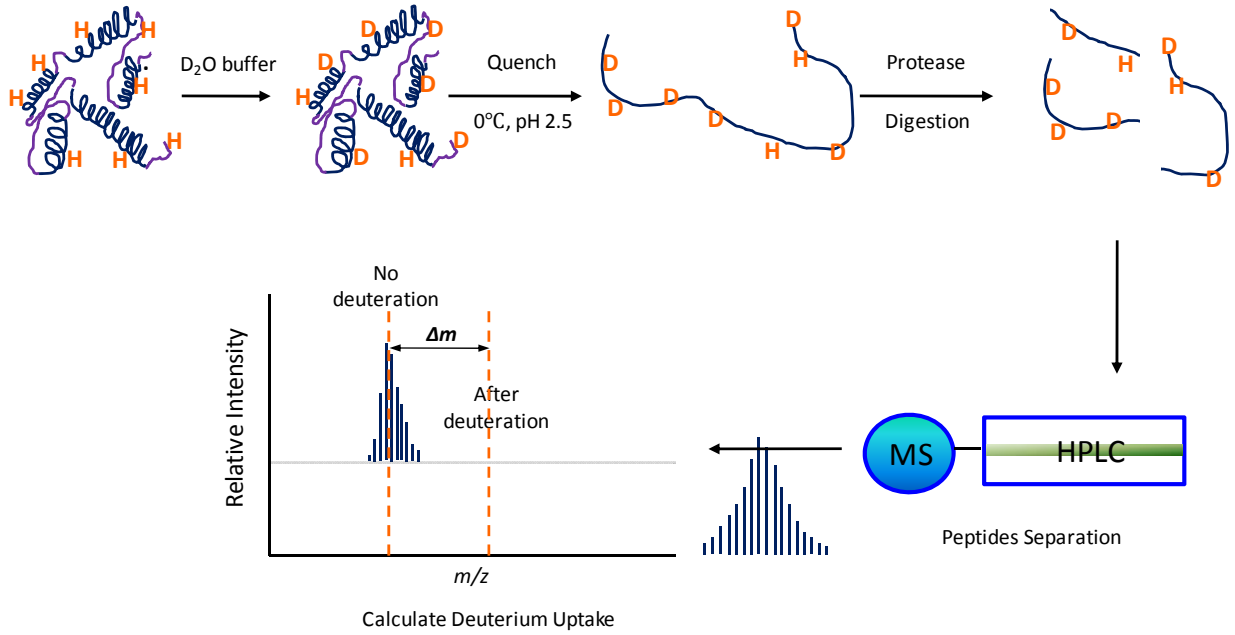

Figure 2-5. Experimental procedure of protein H/D exchange using mass spectrometry

CHAPTER 3
MASS SPECTROMETRIC INVESTIGATION OF MYOGLOBIN IN SOLUTION AND ON NANOPARTICLES

As stated in the previous chapter, the conformation and exchange kinetics of myoglobin adsorbed on silica nanoparticles have been studied using FTICR MS. Pepsin was used as the protease, and peptide fragments including amino acid residues 1-29, 30-69, 70-106, and 107-137 were analyzed.

In this chapter, mass spectrometric data about myoglobin in solution as well as adsorbed on nanoparticles are presented. First, experiments were carried out with the objective of comparing results to literature values[15]. Second, binding isotherms of protein adsorbed on various nanoparticles were obtained. The objective was to find an appropriate nanoparticle material for the HDEX-MS experiment. After analyzing the binding isotherms, pepsin and protease type XIII were used as the proteases. Results of peptide sequence mapping are presented in this chapter.

Sequence Mapping and H/D Exchange of Myoglobin in Solution

This section reports the results of experiments in which myoglobin in solution was analyzed using ESI-Q-TOF mass spectrometry. Protein peptide sequence identification results showed similarity to literature values[15], and reproducible coverage was also obtained. Although the results were similar to those in the reference, the peptide sequence was a little different, because a myoglobin from a different species was used.

Experimental Section

Materials

Myoglobin from equine skeletal muscle was purchased from Sigma Aldrich. Porcine gastric pepsin A was purchased from Biochemical Corporation. 5 mM HEPES

(N-2-hydroxyethylpiperazine-N'-2-ethanesulfonic acid) solution (Fisher Biotech) was used as the buffer, pH 6.5. Heavy water was 99.9% D_2O (Sigma Aldrich).

Instrument

The ESI-Q-TOF mass spectrometer was a QStar XL (Applied Biosystems) equipped with an ion spray source and using N_2 as the nebulizing and desolvation gas. The applied cone voltage range was from 2000 to 2500 V, and no source heater was needed. The scanned range was from m/z 400 to 1500, and samples were scanned for 1 minute (60 total scans) or 2 minutes (120 total scans).

Procedure

Myoglobin in solution: First, 100 µL of 50 µM myoglobin in 5 mM HEPES was digested with 650 µL of 6 µM pepsin in 6% acetic acid for 2 minutes at 0℃. Then 650 µL of ice-cold methanol was added, and the sample was introduced into the mass spectrometer. The final myoglobin concentration was 3.6 µM. For comparison, a more concentrated sample was prepared by digesting 100 µL of 300 µM myoglobin in 5 mM HEPES with 650 µL of 36 µM pepsin in 6% acetic acid for 2 minutes at 0℃, then 650 µL of ice-cold methanol was added and the sample was introduced into the mass spectrometer. The final myoglobin concentration was 21 µM.

H/D exchange of myoglobin in solution: A 10 µL aliquot of 1mM myoglobin in 100mM HEPES was mixed with 190 µL of D_2O. The mixture was incubated for different lengths of time to allow for H/D exchange. A 10 µL aliquot of this solution was mixed with 65 µL of 6 mM pepsin in 6% acetic acid at 0 ℃ for 2 minutes, followed by the addition of 65 µL of ice-cold methanol. The mixture was infused into the mass spectrometer immediately.

Peptide identification. The MS-fit program with the SwissProt (06/10/2008) database was used to identify the digested peptides of myoglobin with porcine gastric pepsin as the protease. Accession number of myoglobin was P68082. The maximum of the missed cleavages was set up as 15. Monoisotopic masses obtained from the spectra were input into the program to compare with the calculated data with 20 ppm mass error tolerance. (http://prospector.ucsf.edu/prospector/cgi-bin/msform.cgi?form=msfitstandard, last accessed on October 4, 2009).

Results and Discussion

The mass spectrometric reproducibility under different protein concentrations and digestion times was investigated. Full scan spectra and sequence mapping and coverage were compared.

The complete spectra of the digested myoglobin at two concentrations are shown in Figure 3-1. There is no significant difference between the 2 spectra in terms of the position and the relative intensities of the major peaks.

The m/z range from 464 to 476 Da of Figure 3-1 is shown in Figure 3-2. It can be clearly seen that the peak clusters have similar isotopic distribution patterns, and for the most part, the relative intensities among peaks are similar. The 70-103 residue has higher relative intensity in the 21 μM solution than in the 3 μM solution. This may be due to the different rates of digestion among different parts of the chain. In general, however, the concentration does not significantly affect the final spectra.

Figure 3-3 shows peptide residue peaks in the digested myoglobin: residues 1-29, 30-69, 70-106, 107-137, and 138-153. These residues cover the length of the molecule, indicating that the coverage is 100% (a better view of the coverage is shown later in the sequence mapping part) from this spectrum. Some of these residues (1-29, 30-69 and

70-106) were analyzed using HDEX-MS and results were compared with the results of Buijs[15]. For some residues, for example, residue 70-106, smaller fragments (residue 87-106 and 70-86) can be used to study the structure of peptide in higher resolution.

Usually peptide sequence mapping is used to show the percent peptide coverage and the degree of amino acid resolution provided by the enzyme and the analytical method. With higher coverage, a better understanding of the protein's global structure can be obtained. Smaller peptide fragments, on the other hand, can provide much more detailed local structural information. Figure 3-4 shows the peptide sequence mapping of the protein based on the data from the Figure 3-3. The peptides found cover all the sequences of the protein. By comparing both larger and smaller residues (such as 1-29 vs. 1-11 and 70-106 vs. 87-106), more detailed local structural information can be obtained.

The effect of digestion time is shown in Figures 3-5 and 3-6. Figure 3-5 shows the spectra of myoglobin in solution after one (top) and two (bottom) minute digestion times. The spectra showed the difference in terms of peak patterns, but 2 min digestion gave better absolute intensity. The 5 minute sample (Figure 3-6) does not show better signal/noise, but the longer digestion time produced more peptides, due to the limited digestion rate.

The peptide coverages for different digestion times are shown in Figures 3-7 and 3-8. The coverages are about the same for the 1, 2, and 5 min samples. However, when digestion time is longer (5 min), more short residues appear. This indicates that digestion time may be a factor that can be used to control the extent of fragmentation.

Results from H/D exchange experiments on myoglobin in solution are presented in Figures 3-9 through 3-13. Some residues (Residue 1-29, for example) are the same as those examined by Buijs[15], but smaller fragments are also analyzed.

The general trends of mass shifts of isotopic distribution peaks are shown in Figure 3-9, which includes residues as follows: (a) 1-29, (b) 12-29, (c) 30-69, (d) 70-106, (e) 107-137, (f) 138-153. As seen in Figure 3-10, the centroidal masses for all the residues increased with increasing H/D exchange time. When all the residues are compared (Figure 3-11), different mass shift patterns are observed. Residues 1-29 and 30-69 show more hydrogens exchanged than residues 70-106 and especially 107-137, which has a mass increase of less than 1 Da over the 100 minute exchange time. This finding is similar to Buijs' work. Gilmanshin found that parts of the G and H helices (residue 101-148) in myoglobin[48] form an extremely stable core[49], that protects those hydrogens from being exchanged. This can explain the low mass increase of residue 107-137 and part of residue 70-106. In most cases, the mass distribution width (Figure 3-12) also increased with exchange time, as observed by Buijs[15], indicating that deuterium was incorporated into the peptide backbone in a more heterogeneous fashion with longer exchange time.

Exchangeable hydrogens in proteins and peptides can be roughly classified into two groups, according to their relative reactivity toward H/D exchange. One group corresponds to hydrogens which are unprotected or barely protected, including side chain or terminal hydrogens. Some amide hydrogens may also be in this group due to their reactivity. Another group of hydrogens are protected and not easily exchanged. In Buijs' work[15], it was assumed that any hydrogens exchanged within 30 seconds belong

to the first group. Based on this assumption, the mass increase after H/D exchange can be classified in 2 parts, as follows:

$$\Delta M = \theta m_1 + \theta m_2[1 - \exp(-k_{ex}t)] \quad (3\text{-}1)$$

In equation 3-1, total mass increase ΔM is due to the exchange from both the first group (with m_1 exchangeable hydrogens) and the second group (with m_2 exchangeable hydrogens). k_{ex} is the exchange rate of the hydrogens in the second group; and θ is the deuterium percentage of all the hydrogens in the solvent. The difference between the total mass increase and the increase from the first group, $\Delta M - \theta m_1$, can be plotted versus the exchange time *t*. The maximum mass increase of this difference, $\Delta M - \theta m_1$, called the relative mass increase, should be θm_2 at sufficient long exchange times. Based on this assumption, the relative mass changes of the 2 residues (1-29 and 30-76) are plotted versus exchange time, as shown in Figure 3-13, which also shows curves simulated using the above formula. The maximum relative mass change, i.e., the value of θm_2, was assigned by assuming 2 factors: (1) the mass increase almost reaches the maximum after 90 minutes of exchange; (2) θm_2 is calculated by multiplying the percentage of deuterium (0.9) in the solvent and an integer, so that the product is close to the maximum mass increase from the experiment. The simulation curve from the reference[15] was calculated based on the data provided in their publication. The rate constants fit to the current work are greater than those in the reference. The average exchange rate constants for residue 1-29 and residue 30-69 are 4.50 h^{-1} and 5.52 h^{-1}, respectively, compared to 0.726 h^{-1} and 4.09 h^{-1} obtained by Buijs. The maximum relative mass increases are smaller than those reported in the reference.

This apparent difference may come from back exchange or experimental error due to the lack of sample replicates in this work.

Binding Isotherms of Myoglobin on Nanoparticles

The purpose of the experiments described in this section was to determine the maximum amount of myoglobin adsorbed on various nanoparticles. The adsorption was assumed to follow the Langmuir model[50].

Experimental Section

Materials

Nanoparticles used for this research were mainly characterized for nominal size, size distribution, and specific surface area. Size distributions of suspended particles were measured using a differential sedimentation CPS Disc Centrifuge™ (CPS Instruments, Stuart, FL). Samples were dispersed in deionized water and phosphate buffered saline (PBS) by 1 minute bath sonication and the resultant particle size distributions were measured by differential sedimentation. BET (Brunauer, Emmett and Teller) surface area was measured using a Quantachrome Autosorb 1C-MS (Quantachrome Instruments, Boynton Beach, FL).

The Co(core)/Co_3O_4 (shell) nanoparticles had a nominal size range of 5 - 20 nm (diameter), and the primary particle size distribution was determined to be 10.5 ± 2.3 nm, with a specific surface area (measured by BET) of 36.39 m^2/g. Silver particles had a nominal size range of 20 - 30 nm (diameter), the primary particle size distribution was determined to be 26.6 ± 8.8 nm, with a specific surface area (BET) of 14.53 m^2/g. TiO_2 had a nominal size of 25 nm (diameter), the primary particle size distribution was determined to be 20.5 ± 6.7 nm, with a specific surface area (BET) of 45.41 m^2/g. Cobalt and silver nanoparticles were purchased from Quantum Sphere (Santa Ana, CA,

USA). TiO_2 was purchased from Degussa (Essen, Germany). Nickel nanoparticles with a nominal diameter of 50 nm and a specific surface area (BET) of 8.15 m^2/g were obtained from Argonide Inc. (Sanford, Florida). Colloidal Au particles with a nominal diameter of 20 nm were synthesized in the Particle Engineering Research Center by reduction of gold chloride with citrate. These particles had particle size distribution of 20 +/- 1 nm (diameter) and calculated specific surface area (BET) of 16 m^2/g.

Procedure for generation of protein adsorption isotherms

Myoglobin solution from equine skeletal muscle (Sigma) and gold ,TiO_2, nickel, silver or cobalt nanoparticles were vortex-mixed in 5 mM HEPES buffer at room temperature for 2 hours and centrifuged for 5 minutes at 18000 rpm (Sigma Centrifuge, Model 1-15). The concentration of free myoglobin (non-adsorbed) in the supernatant was determined by measuring the UV absorbance at 410 nm (Molecular Devices UV/vis spectrometer, Spectramax plus 384, Sunnyvale, CA). The amount of protein adsorbed on nanoparticles was obtained by subtracting the free myoglobin from the initial amount.

Results and Discussion

The adsorption data were fit to theoretical curves, which were calculated based on the Langmuir adsorption model[50]:

$$\frac{A_b}{A_{max}} = \frac{k[c]}{k[c]+1} \quad (3\text{-}2)$$

In equation 3-2, A_b represents the amount of protein binding to nanoparticles, A_{max} is the maximum amount of protein binding to nanoparticles, A_b/A_{max} is the fraction of the particle surface covered, c is the free protein concentration, and k is the Langmuir adsorption constant.

The adsorption isotherms are shown in Figure 3-14. The diamonds represent free protein in solution, and the triangles represent protein bound on nanoparticles. The adsorption generally follows the trend of the Langmuir model, with an asymptote at high concentration. It seems that myoglobin has the best adsorption on cobalt nanoparticles with the least amount of free protein in solution. Nickel is next to cobalt in terms of the adsorption amount.

It can be seen that the size of the nanoparticle and the adsorption maximum don't follow a simple relationship, indicating that particle size is not the only factor affecting the amount adsorbed. In fact, nanoparticles tend to aggregate when suspended in solution. This aggregation increases the size of nanoparticles[51] and decreases the solvent accessible surface area. Other surface characteristics, such as charge, polarity and composition, may all contribute to the adsorption. Interactions between the protein and the adsorbent, such as electrostatic interactions, hydrophobic interactions, and specific chemical interactions also play important roles[4]. The mechanism of selective adsorption of proteins on various adsorbents has been attributed to electrostatic interactions[52].

Mass spectrometric methods were tried for protein adsorbed on each of these nanoparticles. It was found that nickel and silver nanoparticles were better than all others in terms of the mass spectral intensity. For other nanoparticles, the adsorption may be so strong that, even after digestion peptides are not released into solution. Based on the adsorption results, silver and nickel nanoparticles were chosen as the adsorption substrate for further MS analysis in the following two sections. The weight

ratio of protein to nanoparticles was set to 1:40 to achieve the maximum adsorption and strong MS signals.

Pepsin Digestion

In this section, pepsin was used as the enzymatic protease to digest protein in solution and adsorbed on silver and nickel nanoparticles. Mass spectra were obtained on a 4.7 T FTICR mass spectrometer. The objective was to identify digested myoglobin in the above two cases before carrying out H/D exchange experiments.

Experimental Section

Materials

Myoglobin from equine skeletal muscle was purchased from Sigma Aldrich. Porcine gastric pepsin A used as a protease was purchased from Biochemical Corporation. 5 mM HEPES solution (Fisher Biotech) was used as the buffer, pH 6.5. Cobalt, nickel and silver nanoparticles were purchased from QuantumSphere.

Instrument

The instrument used for this study was Bruker 4.7 T FTICR mass spectrometer (Bruker Daltonics, Billerica, MA, USA) in the positive ion mode[53]. Samples were introduced and ionized using an Analytica of Branford electrospray ionization source, with a heated metal capillary (HMC) and a hexapole trapping region. No nebulizing gas was needed in the source. All the samples were directly infused into the ionization source region at a flow rate of 15 μL /hr. The mass range scanned was from m/z 200 to 1500 Da with accumulation of 25 to 100 scans. Ions were produced by the application of a high voltage (~1.5-2.0 kV) to a metal union in contact with the sample solution. The charged solution was pumped toward the HMC, maintained around + 140 V and 120°C. Ions were trapped and accumulated in the hexapole region. After tuning for optimal

transmittance, ions were pulsed toward the ICR cell. Detection was accomplished by collecting the induced image current for 256 K data point transients. After Fourier transformation, the time-domain image current provided the mass spectrum.

Analysis of protein digested with pepsin

In solution. Ten μL of 50 mM myoglobin in 5 mM HEPES was mixed with 65 μL of 6 mM porcine gastric pepsin in 6% acetic acid at 0℃ for 2 minutes. The solution was desalted with C_{18} ZipTips (Millipore) and eluted with 0.1% formic acid in 80:20 acetonitrile:H_2O. The eluate was infused into a 4.7 T FTICR mass spectrometer.

On Ag or Ni nanoparticles. Myoglobin and nanoparticles (1:40) were dissolved/suspended in 5 mM HEPES buffer for 2 hours. The particle part was separated, washed, and digested with pepsin. The supernatant was separated after centrifugation, desalted, and infused into a 4.7 T FTICR mass spectrometer.

Results and Discussion

Mass spectra were obtained after pepsin digestion for myoglobin both in solution and adsorbed on nanoparticles. Peptides in the protein sequence were identified, and the coverage was obtained based on sequence mapping.

Figure 3-15 shows the spectra of the digest in solution and adsorbed on nickel and silver nanoparticles. As can be seen, the general pattern of the spectra is similar. But more small peaks are observed for myoglobin on nanoparticles. For the solution sample, the most intense peak is from the residue 71-107.

In the spectrum for myoglobin on nickel nanoparticles, the 71-107 residue is again the most intense. More small peaks appear, especially in the low mass range below 500. Some fragments, such as residue 71-87 and 59-102, which are not significant in

the spectrum for protein in solution, were identified here. This difference indicates that the adsorption of protein on nanoparticles may affect the digestion pattern or extent.

In the spectrum for myoglobin on silver nanoparticles, there are many small peaks (for example, residues 71-77, 71-87, 59-102), compared to the spectrum of myoglobin in solution. This is similar to the spectrum for protein adsorbed on nickel particles. The 71-107 residue peak is very intense, but the most intense peak corresponds to the 139-154 residue.

Fig. 3-16 compares peptide coverage of myoglobin in solution, adsorbed on Ni and adsorbed on Ag after 2 minutes digestion by pepsin. The sequence coverage for myoglobin in solution was 95% while the coverages for myoglobin bound to Ni and Ag nanoparticles were 93% and 87%, respectively. The sequence maps are similar for the three cases. But there are also different fragments observed for myoglobin adsorbed on nanoparticles, in particular, residues 59-102 and 71-87. These results indicate that adsorption on nanoparticles may change the fragmentation mode of protein upon pepsin digestion.

Protease XIII Digestion

In this section, protease type XIII was used to digest protein in solution and adsorbed on silver nanoparticles. Mass spectra were obtained on a 14.5 T FTICR mass spectrometer. The objective was to identify digested myoglobin in the above two cases before carrying out H/D exchange experiments.

Experimental Section

Materials

Apomyoglobin from equine skeletal muscle and protease XIII from Aspergillus saitoi were purchased from Sigma Aldrich. Silver nanoparticles were purchased from

QuantumSphere. 20 nm alumina membrane syringe filters were purchased from Whatman.

Instrument

The instrument used for this study was a hybrid LTQ 14.5 T FTICR Mass Spectrometer (Thermo Electron Corp., San Jose, CA) custom-built at the National High Magnetic Field Laboratory (NHMFL)[54]. The instrument was operated in the positive ion mode, and the mass range scanned was from m/z 400 to 1600 Da.

Analysis of protein digested with protease XIII

In solution. A 50 µL aliquot of 8 pmol/µL apomyoglobin (0.136 mg/mL) in 50mM sodium phosphate buffer, pH 7.8, was mixed with 50 µL of 1.492mg/mL protease XIII in 1.0% formic acid at 0℃ for 2 minutes. The mixture was desalted and analyzed with the 14.5 T FTICR mass spectrometer at the NHMFL.

On Ag nanoparticles. A 100 µL aliquot of 80 pmol/µL apomyoglobin (1.36 mg/mL) in 50mM sodium phosphate buffer, pH 7.8, was added to 2.72 mg of Ag nanoparticles (20-30 nm, QuantumSphere) and rotated for 5 hrs. The particle part was separated, washed and digested by 500 µL of 1.492 mg/mL protease XIII solution in 1.0% formic acid at 0℃ and vortex-mixed for 2 minutes to prevent precipitation. The supernatant was separated with 20 nm syringe filters, desalted, and infused into the 14.5 T FTICR mass spectrometer at the NHMFL.

Results and Discussion

Figure 3-17 shows the mass spectrum with a charge state distribution of intact apomyoglobin in solution. Analysis of the change of the charge state distribution may help study the conformational changes of protein; however, this is not the focus of the research.

The peptide coverage and sequence mapping shown in Figure 3-18 correspond to apomyoglobin in solution and adsorbed on Ag nanoparticles with 2 min digestion using protease XIII. The sequence coverage for apomyoglobin in solution is 85.6% while that for apomyoglobin bound to Ag nanoparticles is 84.3%. This coverage is about the same as seen in the previous section, but pepsin seems to give a somewhat higher coverage. By using protease type XIII, however, very small fragments containing as few as 2 amino acid residues (such as residue 104-105) can be obtained. This will be beneficial when studying local structural stability, because it will be possible to obtain structural information at the several amino acid residue resolution level. The digestion pattern is also different than that observed in pepsin digested samples. Combining these 2 proteases should be very helpful in elucidating protein structure. Other advantages of using protease XIII include increased electrospray ionization efficiency for mass spectrometric detection, increased signal to noise ratio, and lower tendency of self-digestion of the protease[18].

The common fragments for protein in solution and on silver correspond to a coverage of 74.5% (Figure 3-19). This implies that it is very promising to study globally, as well as locally, the conformational changes of myoglobin adsorbed on nanoparticles by comparing the mass spectrometric data for these common fragments.

Summary

As a summary of this chapter, the following statements can be made:

- H/D exchange of myoglobin in solution was performed and results were compared with reference data;
- Binding isotherms of myoglobin adsorbed on nanoparticles were obtained;
- Myoglobin in solution was digested with pepsin and protease XIII and peptide sequences were mapped;

- Myoglobin adsorbed on nanoparticles (Ni, Ag) was digested with pepsin and protease XIII and peptide sequences were mapped;

- Protease XIII provides different fragmentation patterns for myoglobin than pepsin, suggesting a promising way of studying both global and local structure of myoglobin by mass spectrometry.

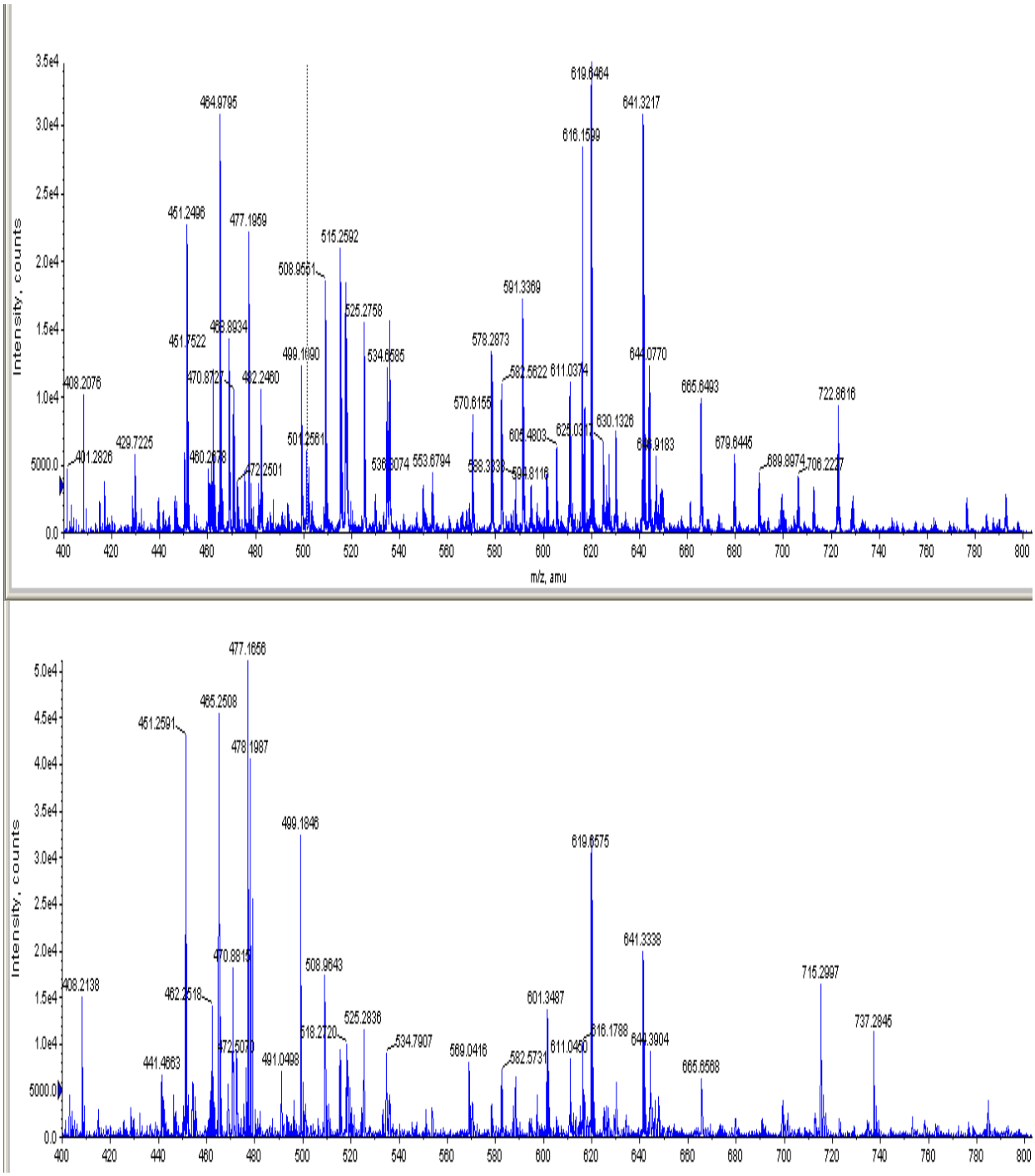

Figure 3-1. Mass spectra of myoglobin in solution obtained with ESI-Q-TOF: top: 21 μM; bottom: 3.6 μM

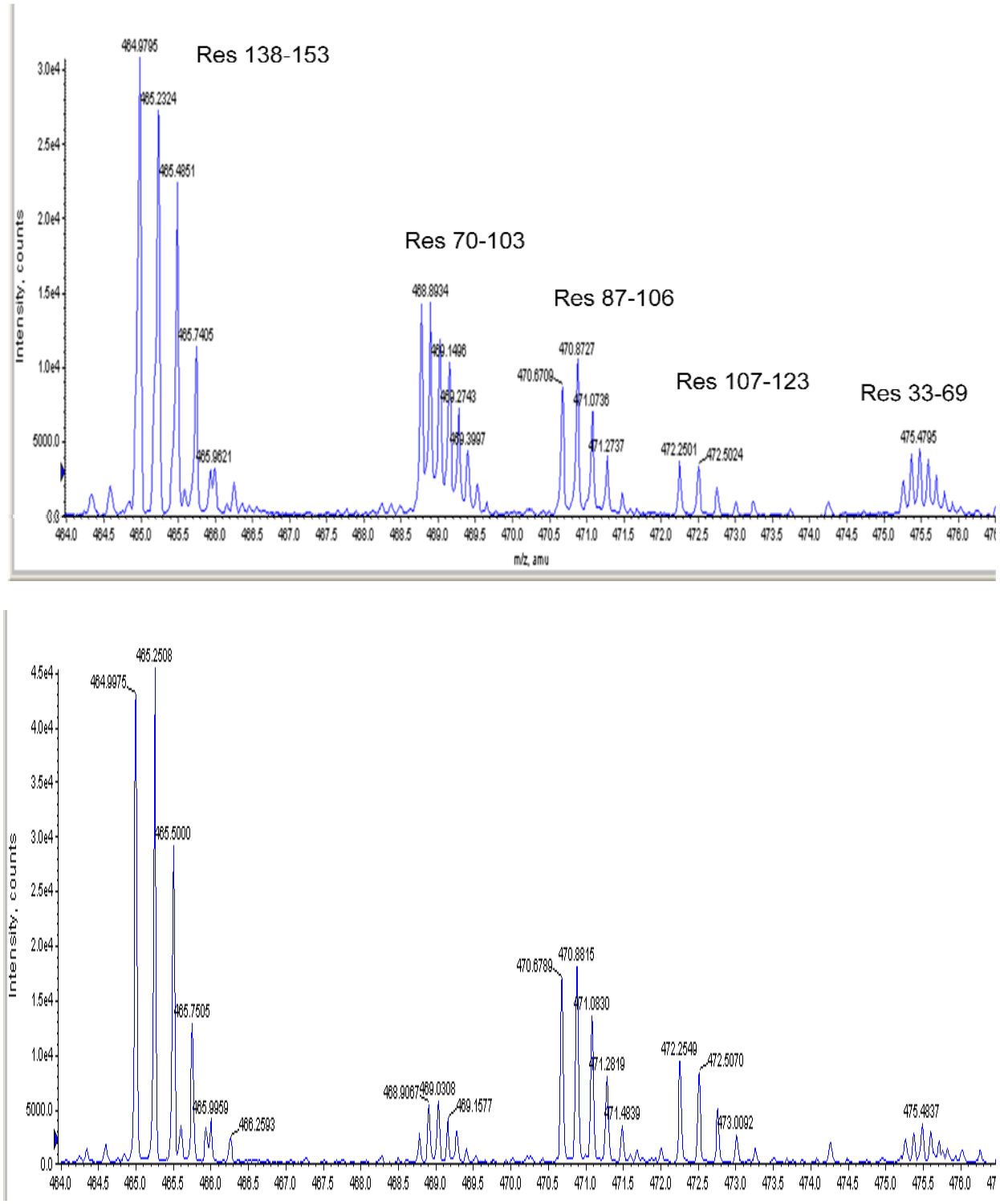

Figure 3-2. Expansion of 464 to 476 m/z region of Figure 3-1

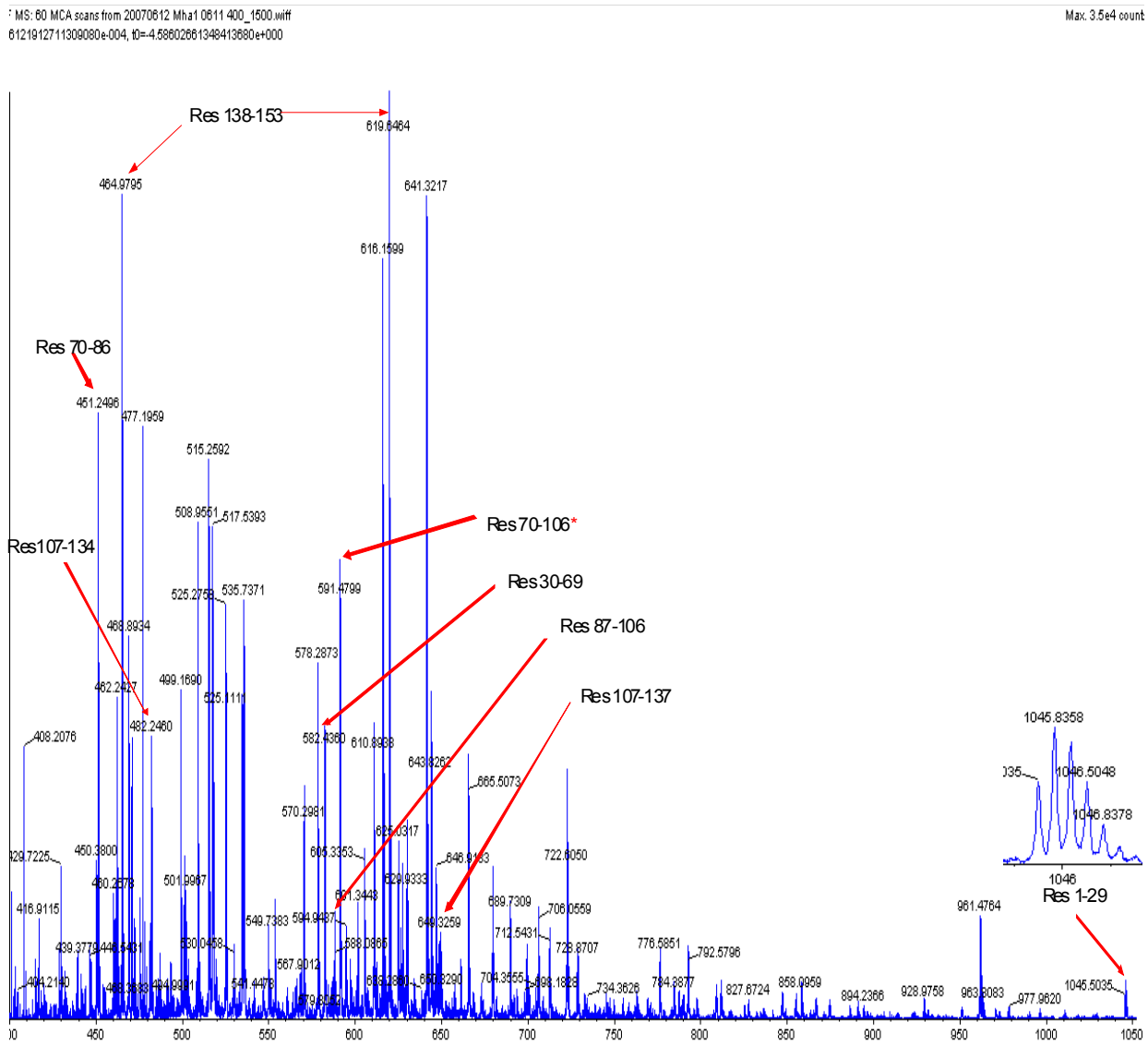

Figure 3-3. Mass spectrum of 3.6 μM myoglobin in solution, the same as the bottom of Figure 3-1, with labeled residues. *: For residue 70-106, smaller residues of it (residue 70-86 and 87-106) can be used to study the structure of the peptide in higher resolution

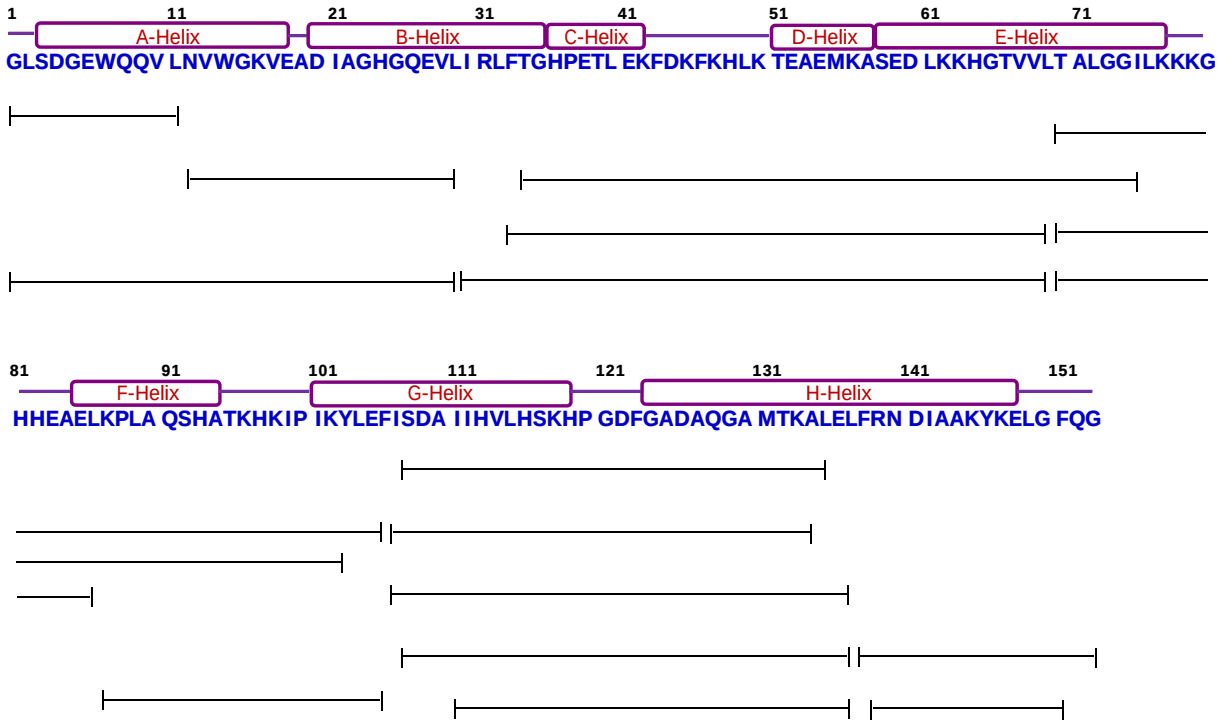

Figure 3-4. Peptide coverage obtained with 3.6 µM concentration of myoglobin

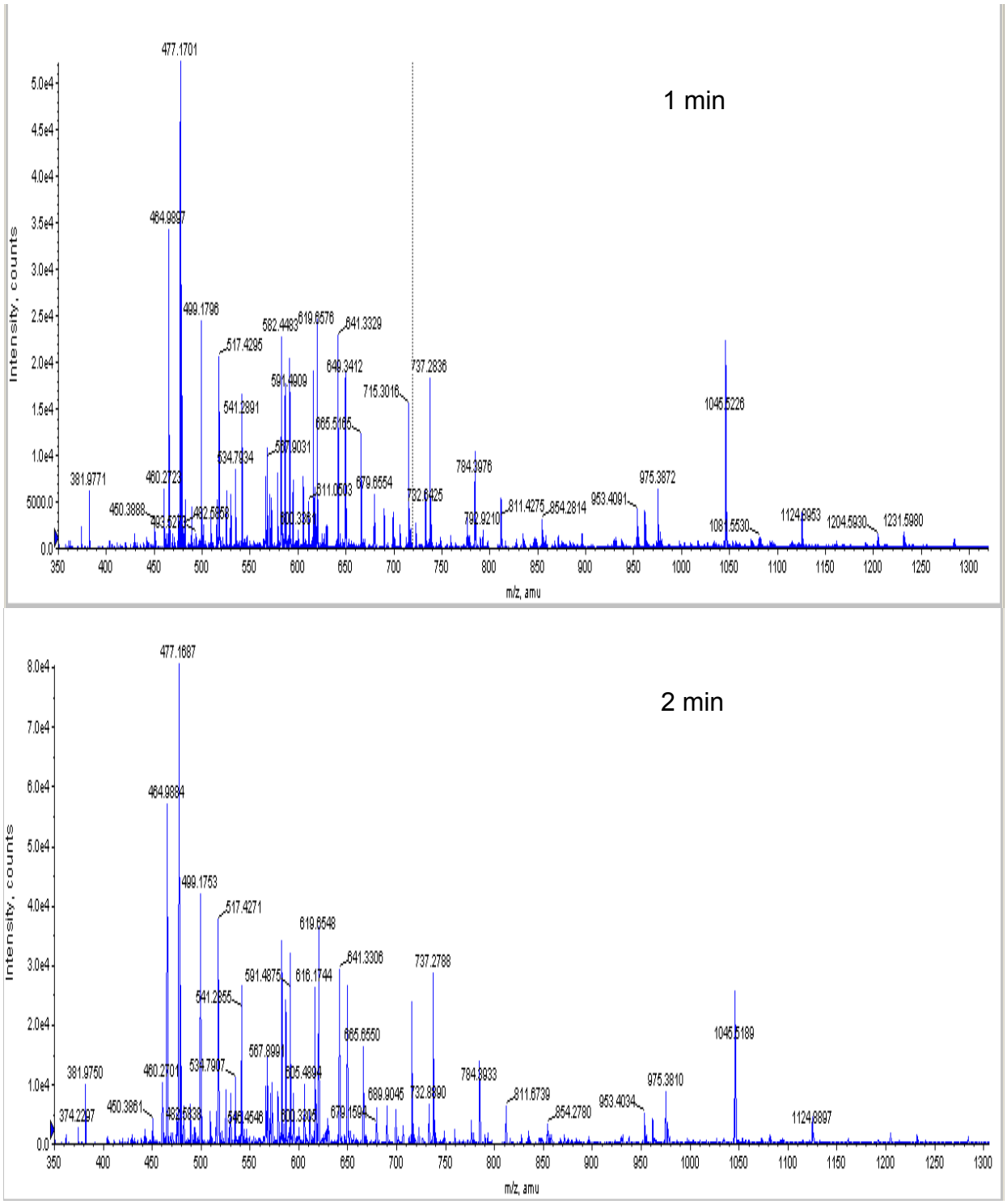

Figure 3-5. Mass spectra of myoglobin in solution obtained after different digestion times: top: 1 minute; bottom: 2 minutes

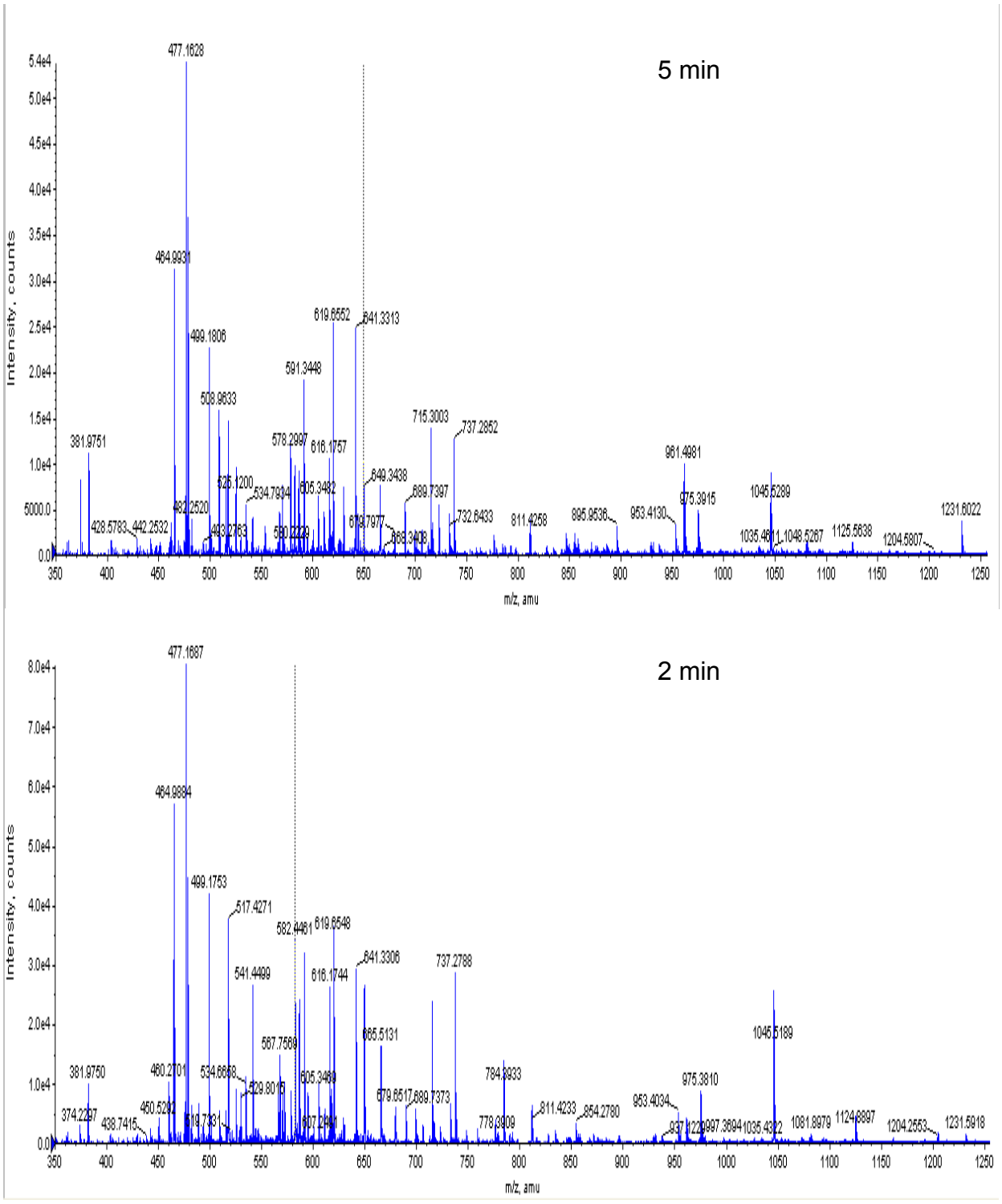

Figure 3-6. Mass spectra of myoglobin in solution obtained after different digestion times: top: 5 minutes; bottom: 2 minutes

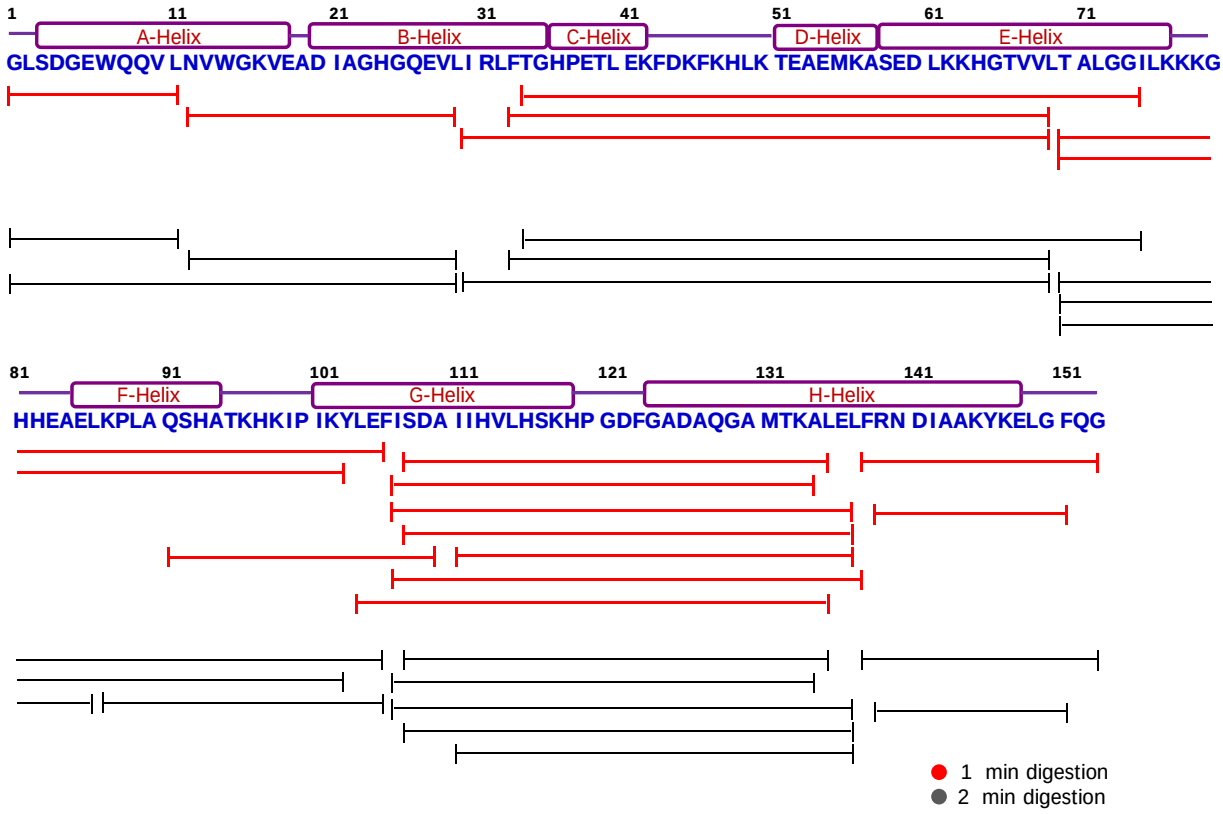

Figure 3-7. Comparison of peptide coverage after different digestion times: top: 1 minute; bottom: 2 minutes

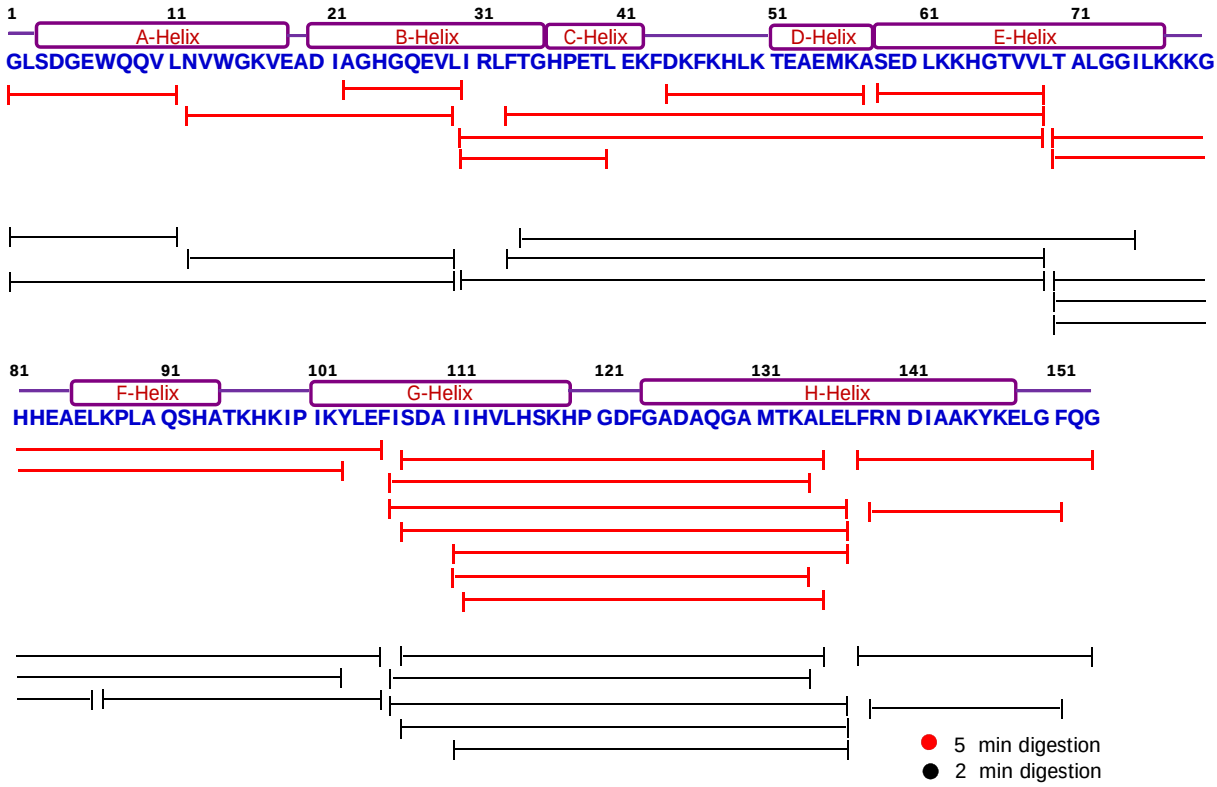

Figure 3-8. Comparison of peptide coverage after different digestion times: top: 5 minutes; bottom: 2 minutes

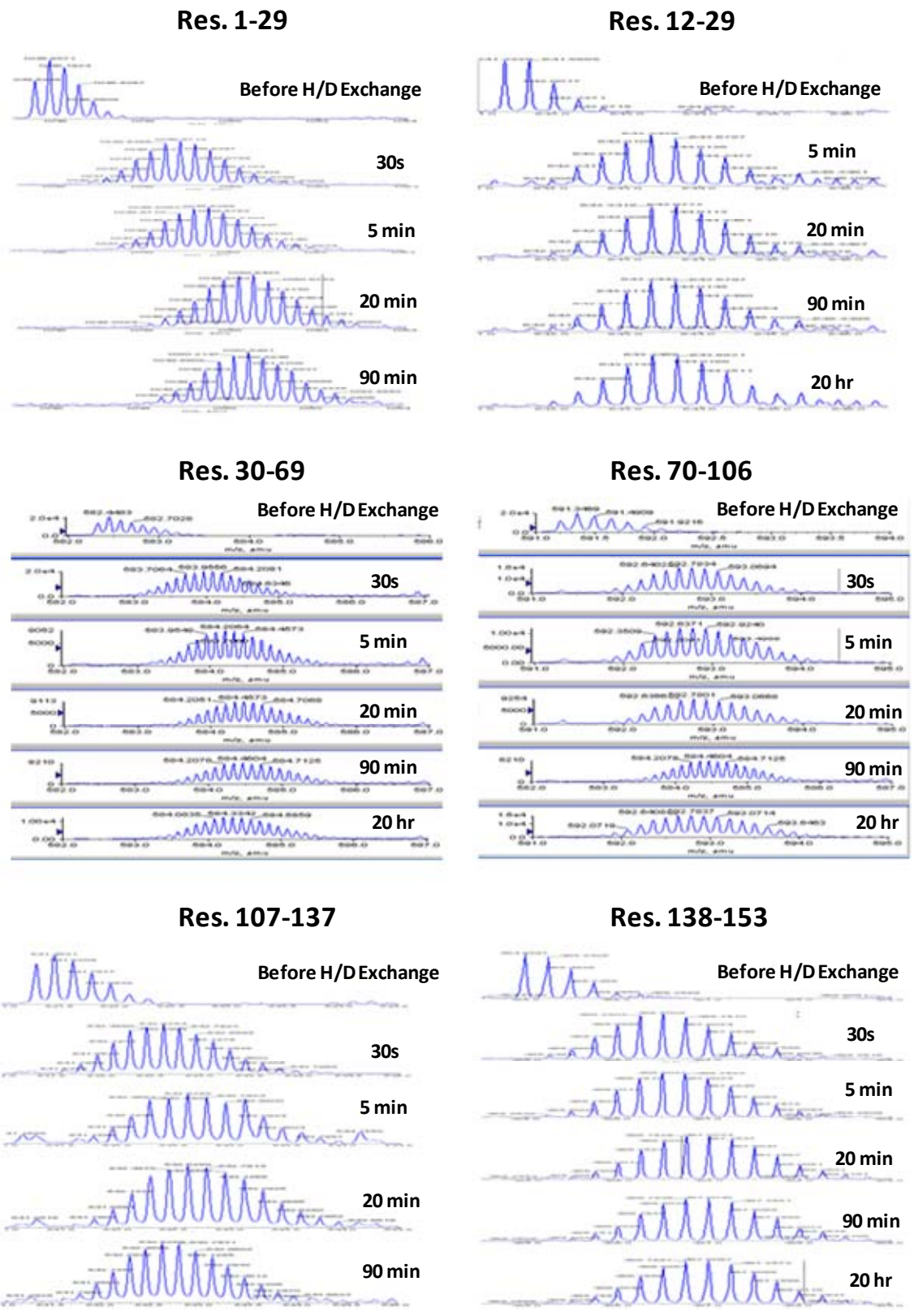

Figure 3-9. Mass spectra showing mass shifts during H/D exchange

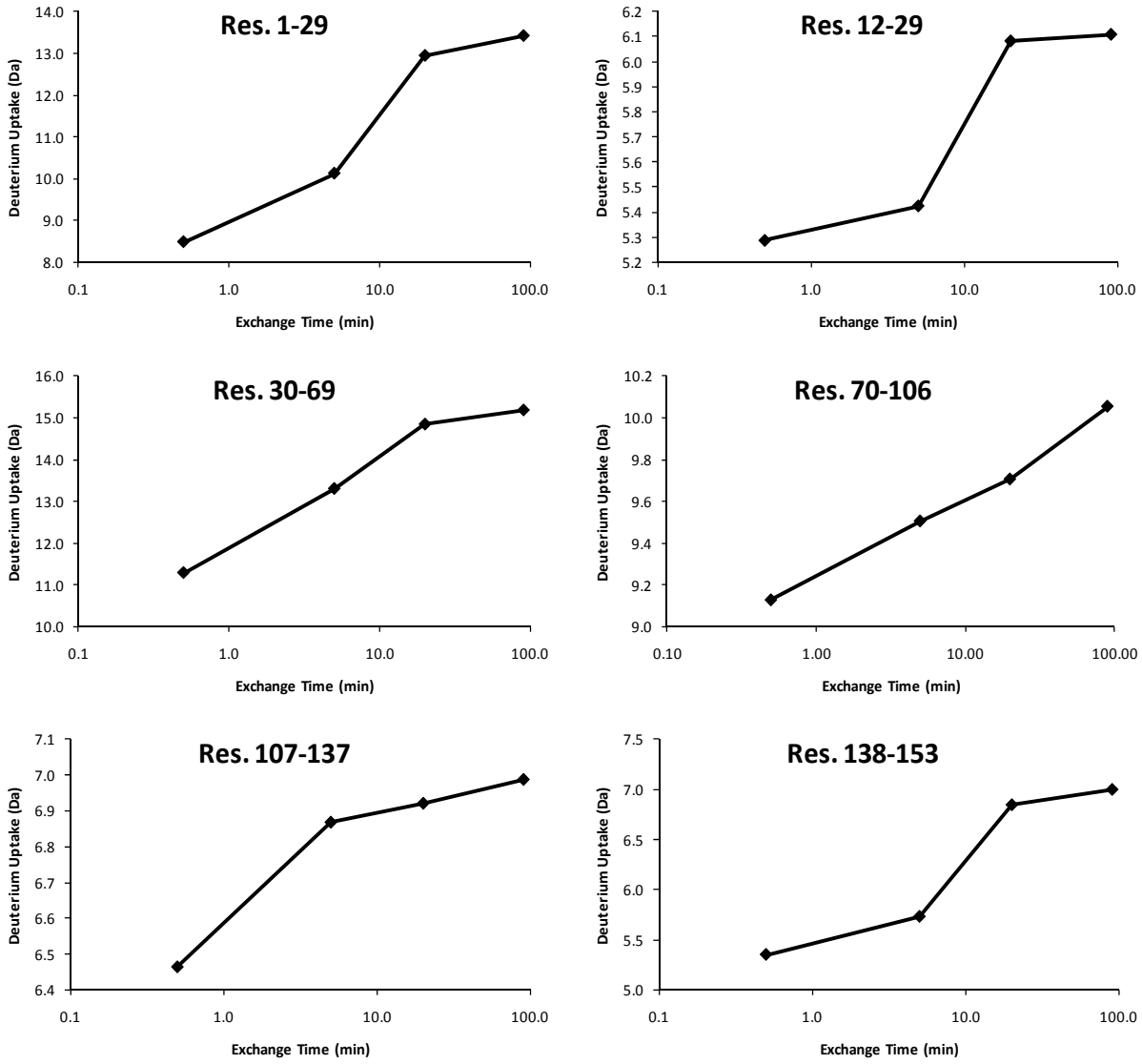

Figure 3-10. Deuterium uptake of various residues in myoglobin in solution

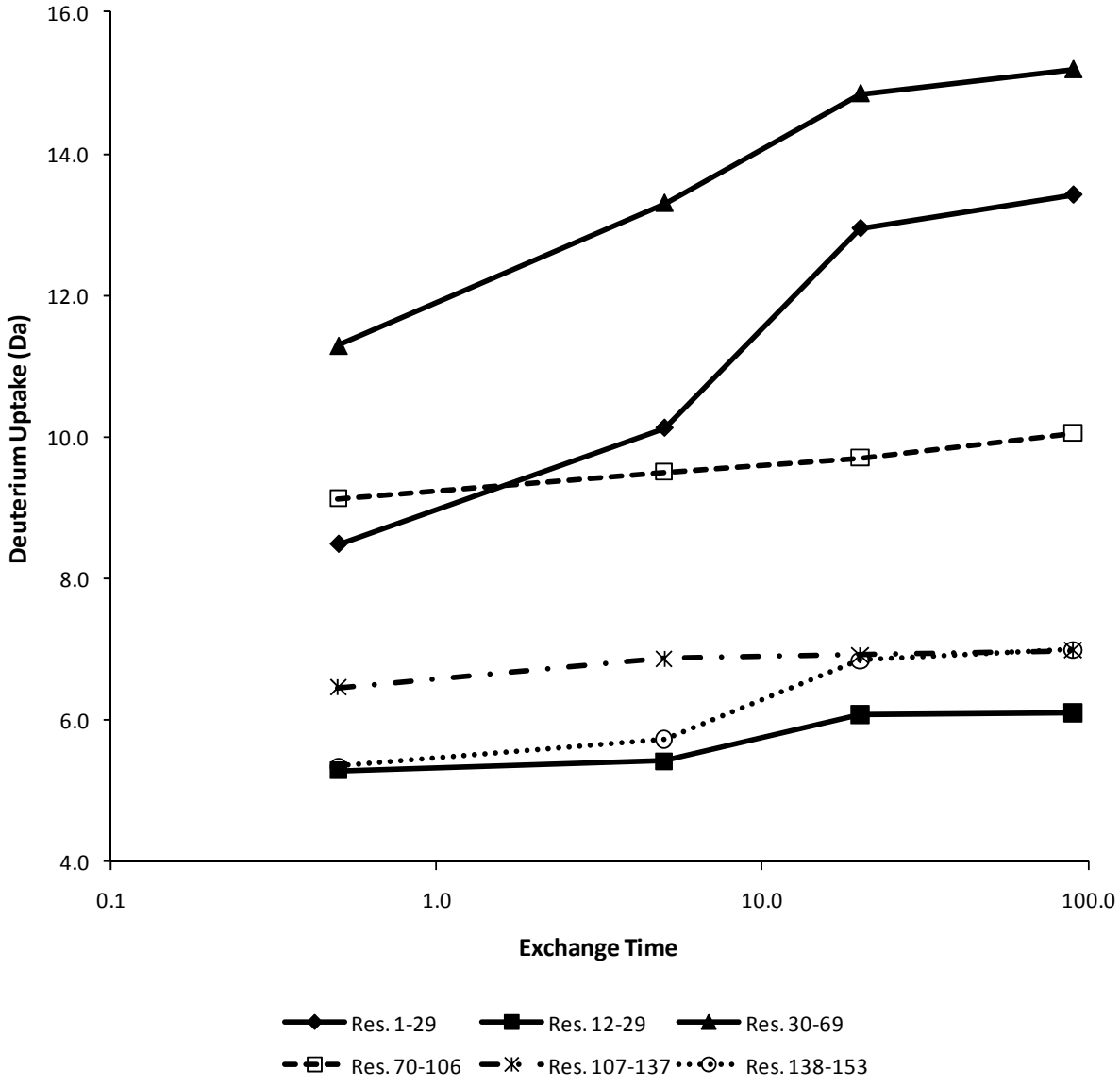

Figure 3-11. Comparison of mass increase for 6 residues

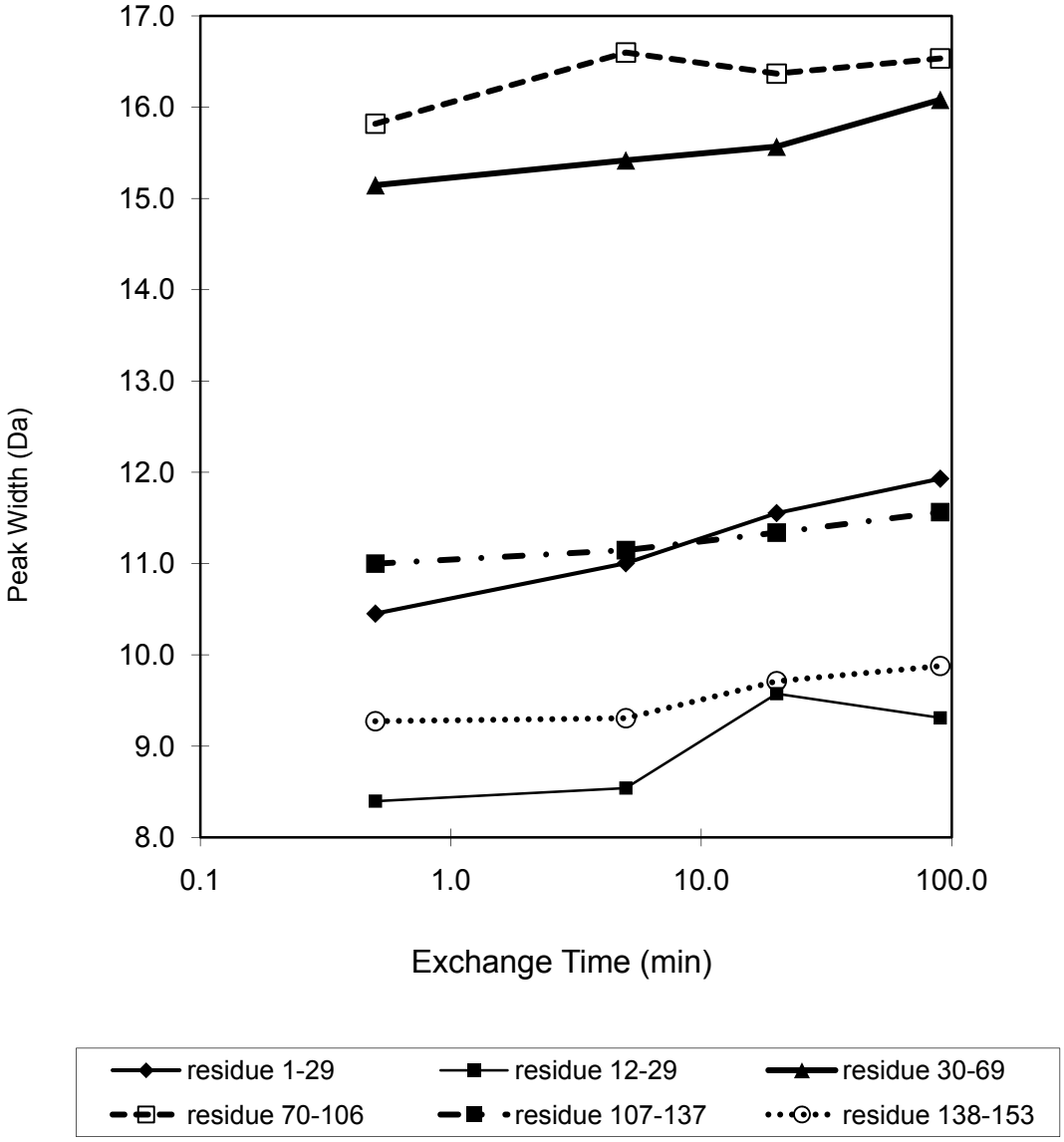

Figure 3-12. Comparison of the change of peak width in H/D exchange

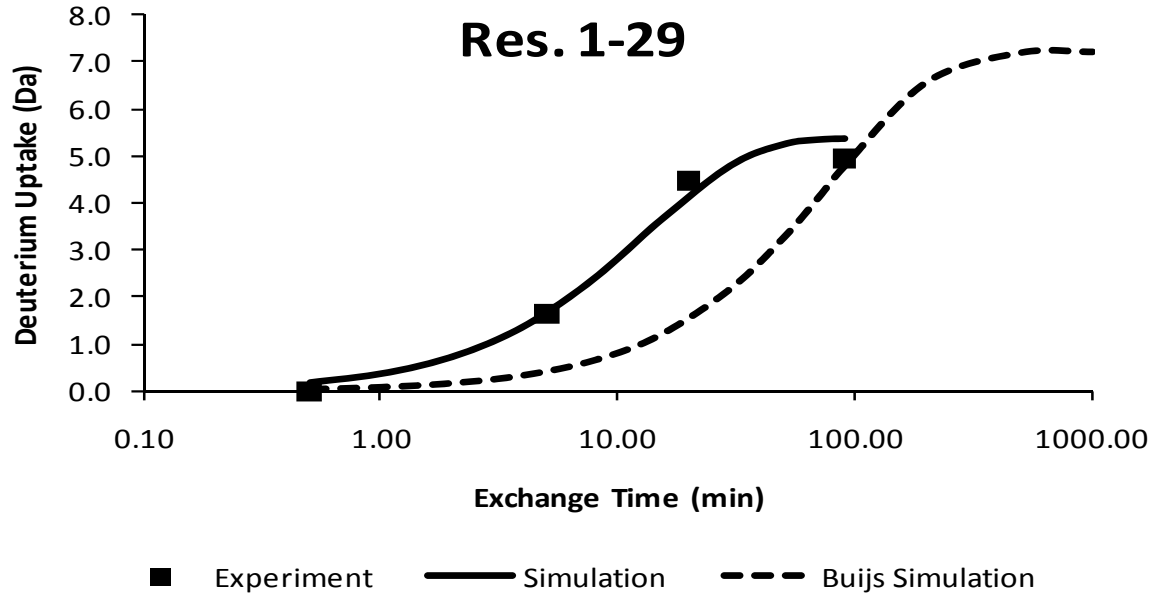

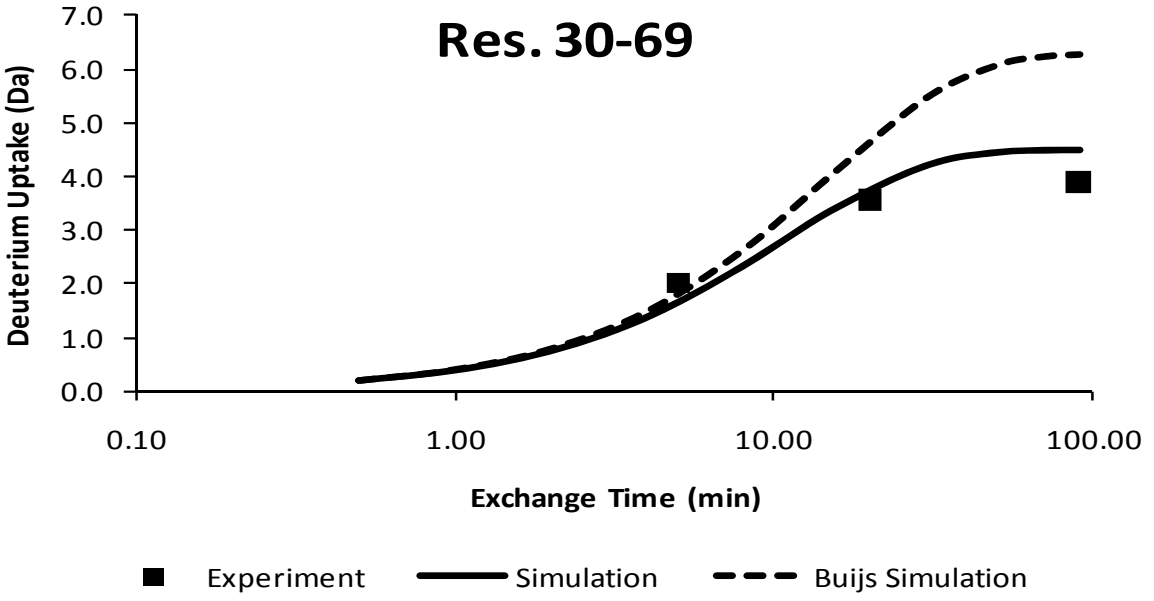

Figure 3-13. Mass increase simulation for residue 1-29 and 30-69

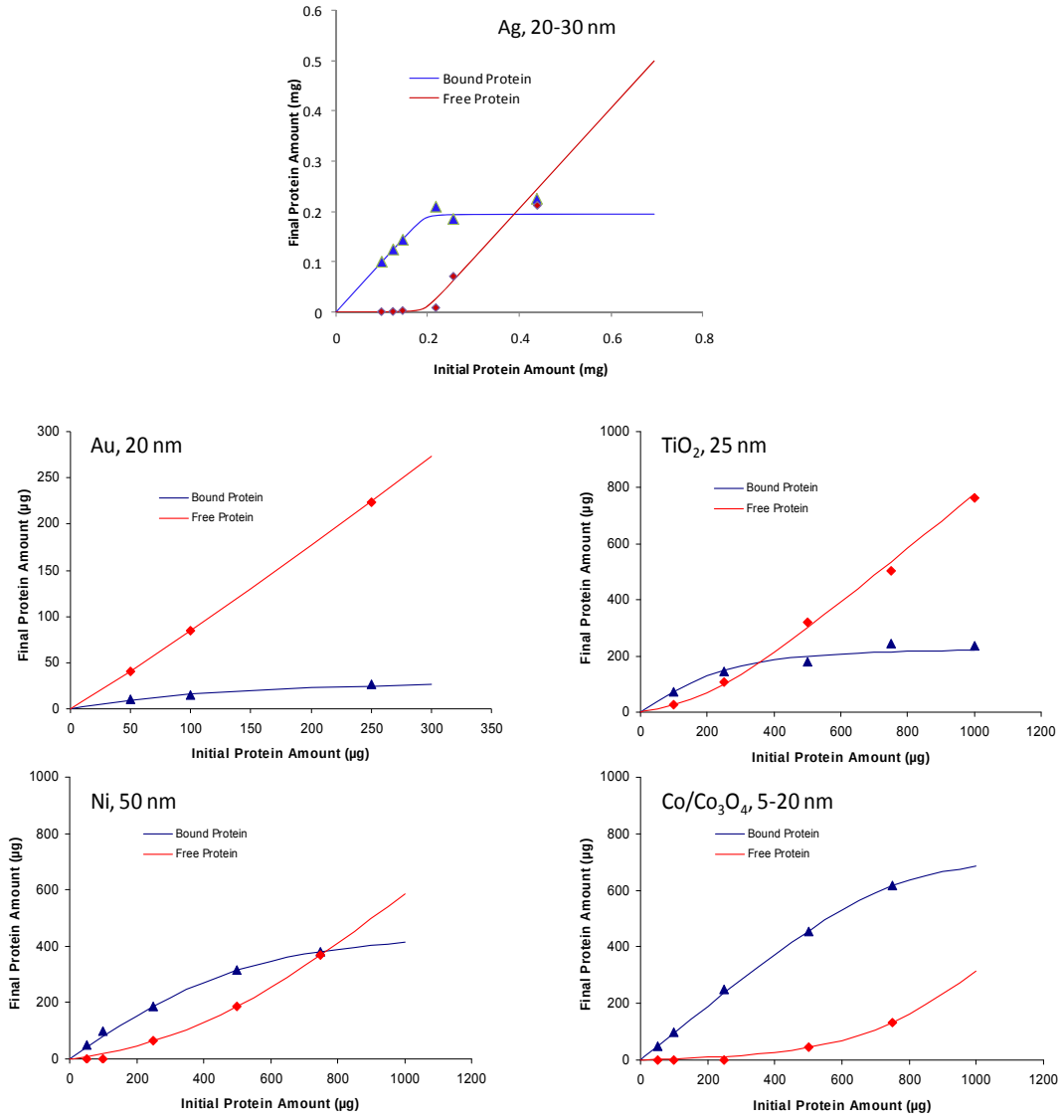

Figure 3-14. Binding isotherms of myoglobin on nanoparticles

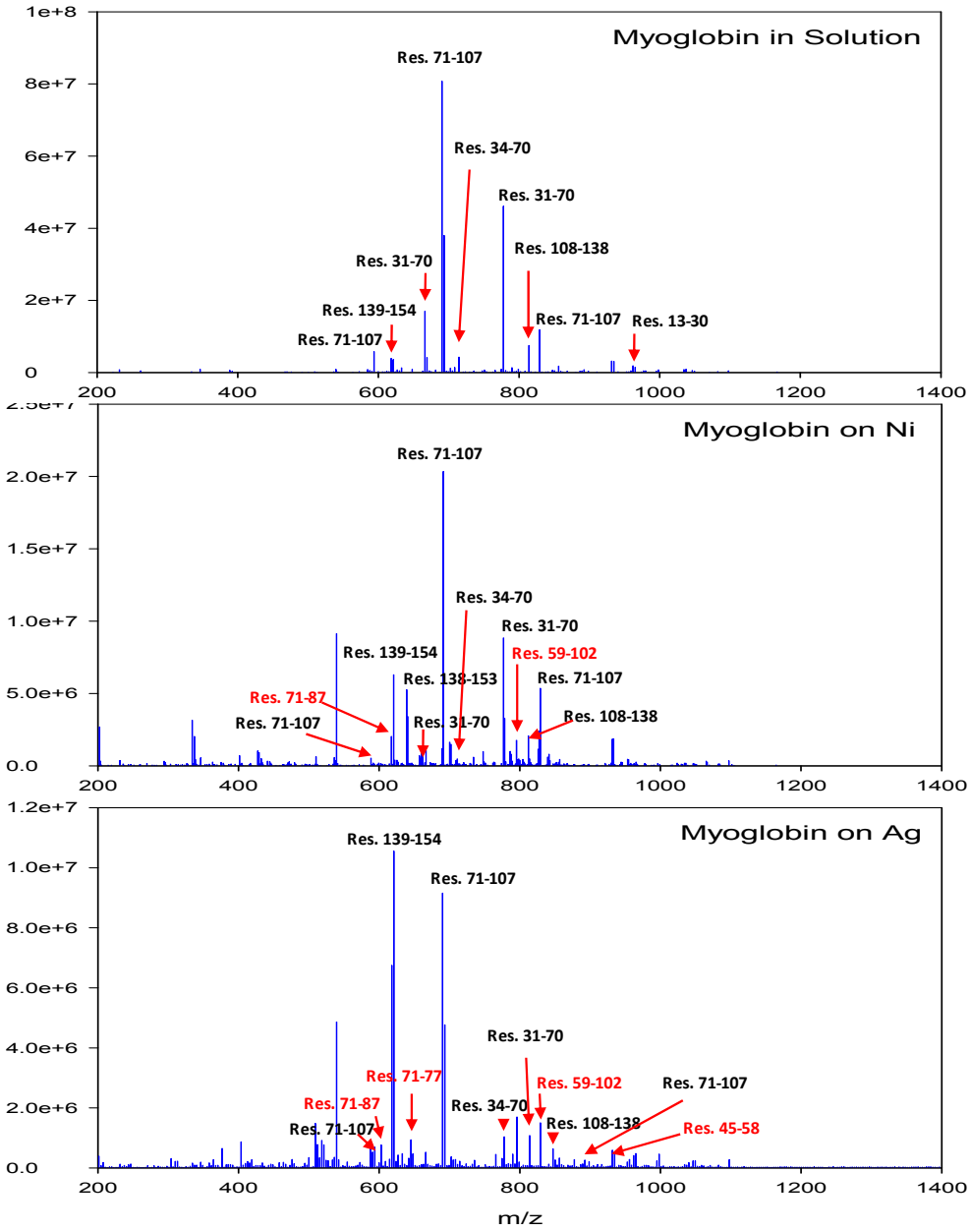

Figure 3-15. Mass spectra of myoglobin digest in solution and on nanoparticles: top: myoglobin in solution; medium: myoglobin binding to nickel; bottom: myoglobin binding to Ag

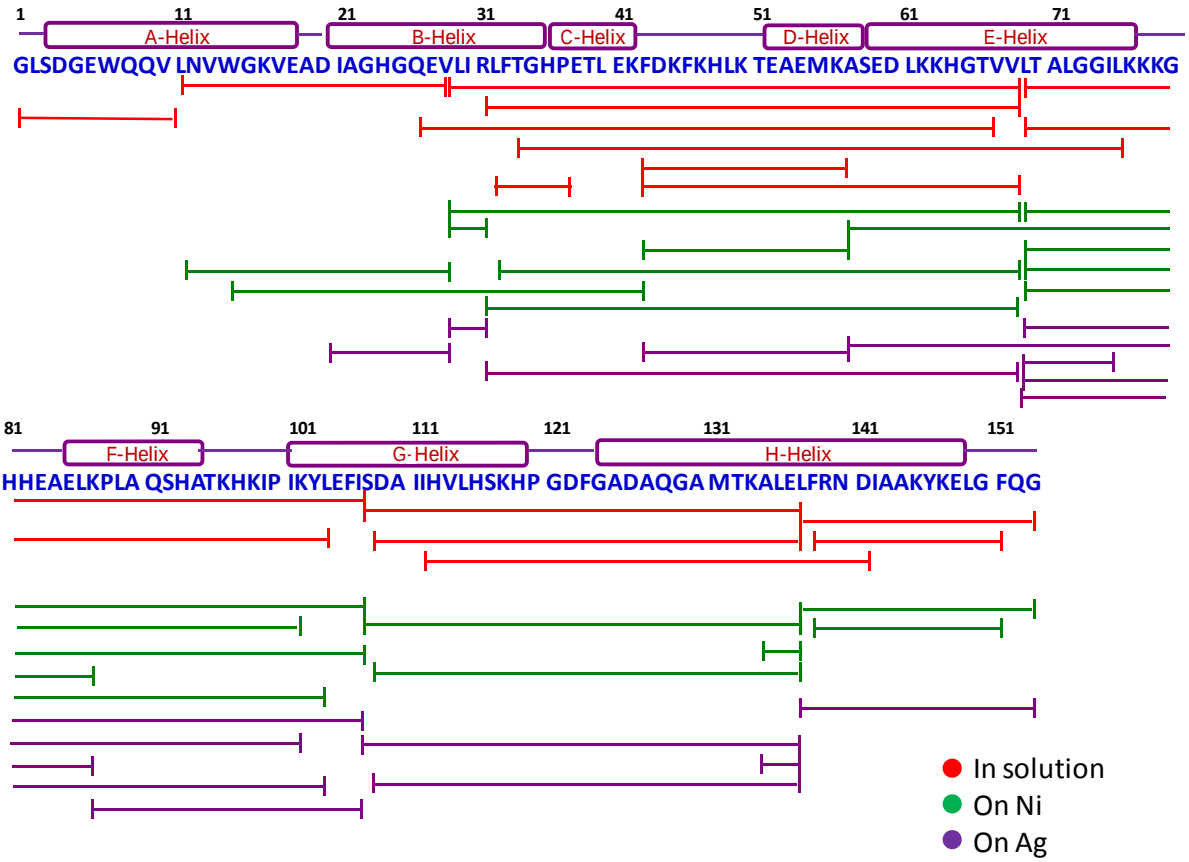

Figure 3-16. Sequence mapping of myoglobin in solution and on nanoparticles, after pepsin digestion

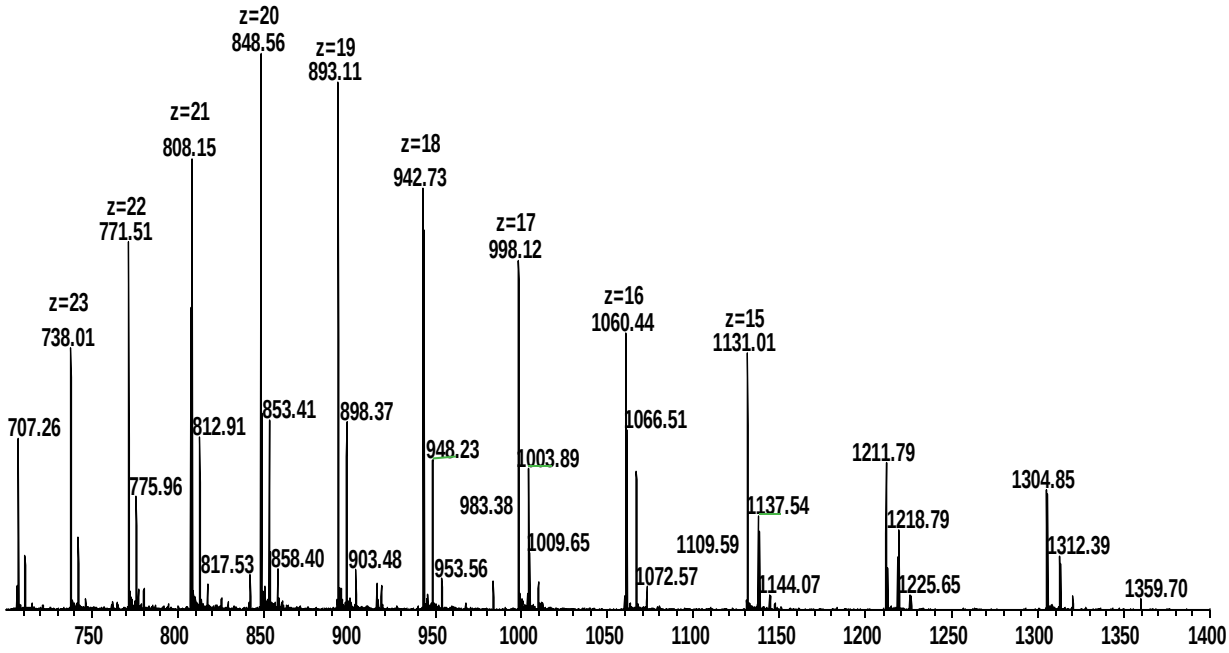

Figure 3-17. Mass spectrum of intact apomyoglobin

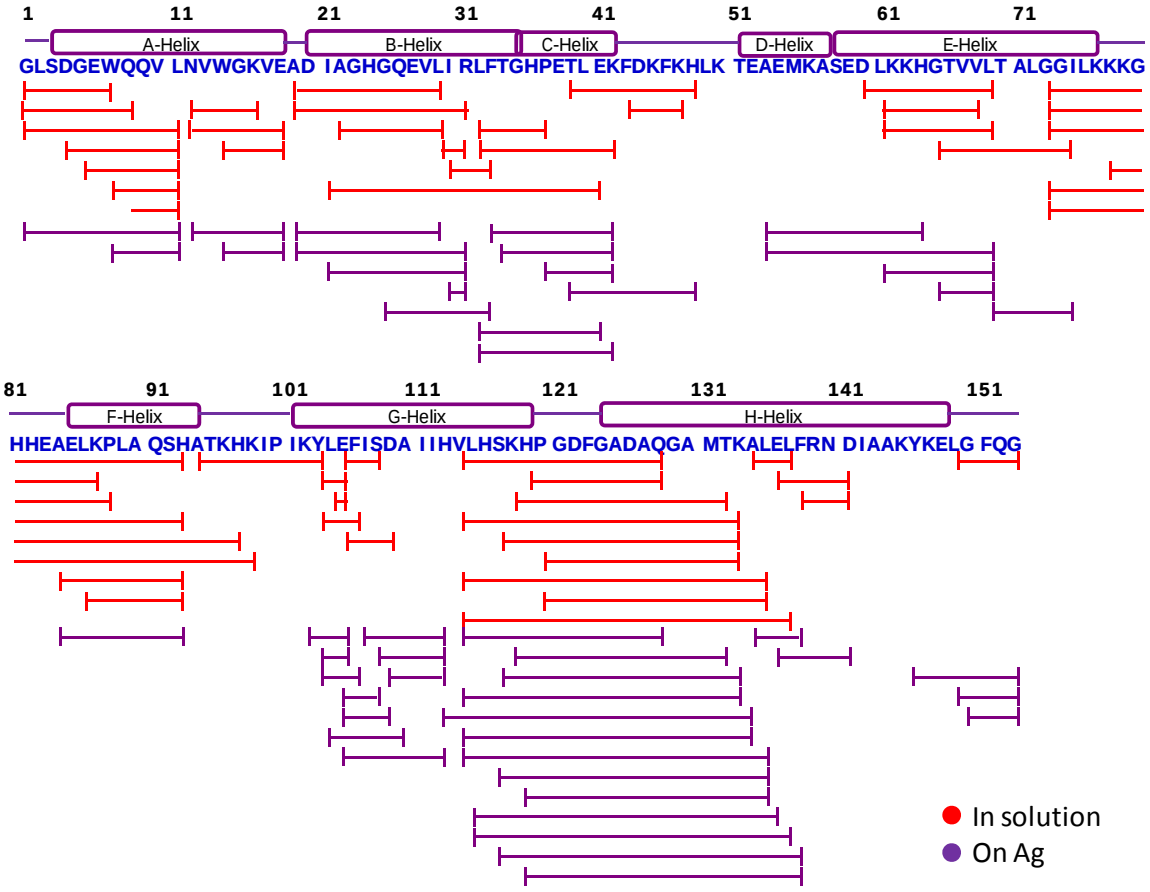

Figure 3-18. Sequence mapping of myoglobin in solution and on silver nanoparticles digested by protease XIII

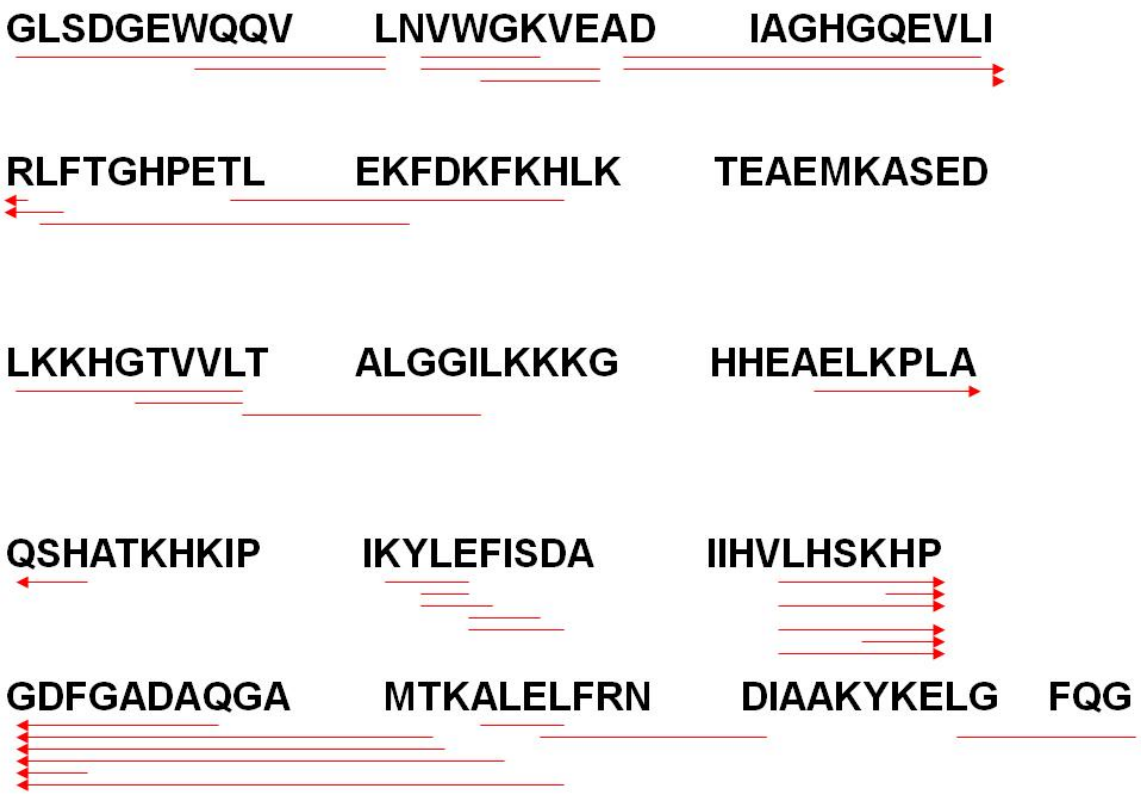

Figure 3-19. Common fragments of myoglobin in solution and on nanoparticles digested by protease XIII

CHAPTER 4
H/D EXCHANGE MASS SPECTROMETRY OF MYOGLOBIN ON SILVER NANOPARTICLES

To achieve the initial goal of investigating protein conformational change during adsorption on nanoparticles, efforts were made to conduct HDEX-MS experiments for myoglobin on silver nanoparticles.

Initially, myoglobin samples (in solution and on silver nanoparticles) after H/D exchange were prepared and sent to the National High Magnetic Field Laboratory (NHMFL) at Florida State University (FSU). Unfortunately, the analysis by HPLC ESI FTICR encountered some unknown contamination from the samples and the analysis was discontinued.

Additional experiments were carried out to seek the reasons for the sample contamination. It was found that the filters used to remove the nanoparticles not only adsorbed the digested peptides, but also contaminated the filtrate. Alternative filters were used to eliminate the contamination issue.

Recently, myoglobin samples (in solution and on silver nanoparticles) after H/D exchange were prepared and analyzed using an LTQ-Orbitrap at the University of South Florida (USF).

Analysis for Sample Contamination Source

Sample Preparation for HDEX-MS

Materials

Myoglobin from equine skeletal muscle and protease XIII from Aspergillus saitoi were purchased from Sigma Aldrich; heavy water was 99.9% D_2O (Sigma Aldrich); 20 nm alumina membrane syringe filters were purchased from Whatman; 200 nm nylon syringe filters were purchased from Fisher; 200 nm Supor membrane syringe filters

were purchased from Pall Gelman Laboratory; Blue plus 2 molecular weight markers were purchased from Invitrogen.

Instrument

The instrument used for this study was a hybrid LTQ 14.5 T FTICR Mass Spectrometer (Thermo Electron Corp., San Jose, CA) custom-built at the National High Magnetic Field Laboratory (NHMFL), also described in Chapter 3. The instrument was operated in the positive ion mode, and the mass range scanned was from m/z 400 to 1600 Da.

H/D exchange mass spectrometry of protein in solution

Aliquots of 10 μL of 80 pmol/μL myoglobin in 50mM sodium phosphate buffer, pH 7.8, were each mixed with 90 μL of 50mM sodium phosphate in D_2O (99.9%, Sigma) buffer, then incubated for different lengths of time to allow for H/D exchange. The sample was then digested with 100 μL of 1.492 mg/mL protease XIII solution in 1.0% formic acid at 0℃ for 2 minutes, filtered with a 20 nm nanofilter, frozen in liquid nitrogen, and stored overnight. The samples were thawed and infused into the 14.5 T FTICR mass spectrometer at the NHMFL immediately.

H/D exchange mass spectrometry of protein on Ag nanoparticles

100 μL of 80 pmol/μL apomyoglobin in 50mM sodium phosphate buffer, pH 7.8, was added to 2.72 mg of Ag nanoparticles (20-30 nm, QuantumSphere) and rotated for 5 hrs. The particle part was separated and washed. 10 μL aliquot of the particle suspension was mixed with 90 μL D_2O and incubated for different lengths of time to allow for H/D exchange. The sample was then digested with 100 μL of 1.492 mg/mL protease XIII solution in 1.0% formic acid at 0℃ for 2 minutes, filtered with a 20 nm

nanofilter, frozen in liquid nitrogen and stored overnight. The samples were thawed and infused into the 14.5 T FTICR mass spectrometer at the NHMFL immediately.

The spectra indicated the presence of a contaminant with very few peptide signals. The source of the contamination was investigated as described below.

Gel electrophoresis analysis for sample contamination

Aliquots of samples (Figure 4-1) were resolved on a 4-12% Bis-Tris-SDS-PAGE gel. Blue plus 2 was used as a standard. Pure myoglobin and protease XIII were analyzed as blank controls. After electrophoresis, the gel was fixed in 50% methanol and 7% acetic acid for 30 minutes twice, stained with Sypro Ruby gel stain overnight, washed with 10% methanol and 7% acetic acid for 30 minutes, then washed with H_2O twice. The gel was analyzed with a UV trans-illuminator (Bio-Rad laboratories, Universal Hood II, CA).

Results and Discussion

In an effort to understand why the samples previously sent to the NHMFL appeared to have poor digestion efficiency, SDS-PAGE analyses were conducted on newly digested samples as well as several samples sent to the NHMFL. The samples included 11 freshly made digests and 2 samples sent to the NHMFL.

Figure 4-1 shows the image of the digested myoglobin samples. Samples in lanes 2-5 were not filtered. Samples in lanes 6-14 were filtered with a 20 nm filter. Samples were separated on 4-12% Bis-Tris gel and stained with Sypro Ruby.

Sypro Ruby protein gel stain is a sensitive fluorescent stain that is used in polyacrylamide gel electrophoresis (PAGE) to detect separated proteins. It has a detection limit of ~ 1ng/band, so there appeared to be very little undigested protein in any of these samples. However, there appeared to be very little protein of any type in

the samples, as bands corresponding to protease XIII were also absent. This was surprising, so another experiment was conducted to evaluate the digestion of myoglobin over time, as well as the impact of 20 nm filtration on the samples. Samples were analyzed on 4-12% Bis-Tris gel with Sypro Ruby staining. The image is shown in Figure 4-2.

From these results, two things are apparent. Protease XIII digestion for 2 minutes appears to digest well over 95% of intact myoglobin. However, 20 nm filtration causes dramatic loss of both myoglobin and protease XIII, likely accounting for the results observed above. Because peptides could not be observed in this analysis, it was unclear how filtration was affecting peptide concentrations, though it is likely that the peptides were also significantly reduced.

It is necessary to remove nanoparticles prior to LC analysis to avoid plugging the column. However, it was shown from the PAGE analysis that the 20 nm filters were not appropriate for preparing samples that would subsequently be analyzed for proteins and peptides. Because significant aggregation of silver particles occurs under conditions of myoglobin binding, 200 nm nylon filters were next investigated (Figure 4-3).

These results demonstrated that 200 nm nylon filtration produced much better protein yields. However, when digests were analyzed by MS, high concentrations of contaminants were identified. These could not be removed by washing the filter with aqueous or organic solvents as evident in Figure 4-4, which shows the MS spectra obtained from myoglobin digests filtered with 200 nm nylon filters.

Analysis of the blank sample presented in Figure 4-4 indicates the presence of strong peaks at 679.4, 701.4 and 717.4 (m/z) in the blank sample after filtration. These

peaks do not appear in the solution without filtration, suggesting that the contamination originated from the nylon filter. These are more evident on the bottom panel of Figure 4-5. The m/z range on the top is from 200 to 1600, and on the bottom is from 678 to 724, which shows an expansion of the m/z region.

Because of the contamination found in nylon filters, alternate filter materials were investigated. It was found that 200 nm Supor membranes did not adsorb sample and did not leach contaminants. These filters were used to conduct an abbreviated H/D exchange experiment, in which samples were analyzed by direct infusion of digests on an LTQ-Orbitrap at USF. As evidenced in the spectra in Figures 4-6 through 4-7, large numbers of peptides were present in these samples, although some of the peptides were quite large (>3500amu), which may indicate incomplete digestion. Figure 4-6 provides an example of the spectra collected by direct infusion of myoglobin digests.

To ensure that enzymatic activity was maximal, a new bottle of Protease XIII was purchased and digestion effectiveness was again determined by SDS-PAGE (Figure 4-8). From Figure 4-8, it is apparent that the new protease XIII enzyme also removes >95% of intact myoglobin after 2 minutes digestion. These results seem very similar to those obtained with the Protease XIII used in prior experiments. Following filtration with 200 nm Supor membranes (lanes 10-13), very little intact myoglobin is visible while the protease XIII concentration appears unaffected.

HDEX-MS of Myoglobin using LTQ-Orbitrap

Experimental Section

Materials

Myoglobin from equine skeletal muscle and protease XIII from Aspergillus saitoi were purchased from Sigma Aldrich; heavy water was 99.9% D_2O (Sigma Aldrich); 200 nm Supor membrane syringe filters were purchased from Pall Gelman Laboratory.

Instrument

The instrument used for this study was an LTQ-Orbitrap mass spectrometer (Thermo Electron Corp., San Jose, CA) at the University of South Florida. The instrument was run in the positive ion mode, with the m/z range scanned from 235 to 2000 Da.

Analysis of protein digested with protease XIII

In solution: a 100 µL aliquot of 16 pmol/µL myoglobin (0.272 mg/mL, equine skeletal, Sigma) in 10 mM ammonium acetate buffer, pH 7.2, was mixed with 100 µL of 2.98 mg/mL protease XIII (Aspergillus saitoi, Sigma) in 1.0% formic acid at 0℃ for 2 minutes. The solution was filtered with a 200 nm Supor filter, and immediately frozen in liquid nitrogen. Then 200 µL ice-cold acetonitrile was added to the frozen sample, which was directly infused into an LTQ-Orbitrap mass spectrometer at USF.

On Ag nanoparticles: a 100 µL aliquot of 16 pmol/µL apomyoglobin (0.272 mg/mL) in 10 mM ammonium acetate buffer, pH 7.2, was added to 5.44 mg of Ag nanoparticles (20-30 nm, QuantumSphere) and rotated for 5 hrs. The particle part was separated, washed and digested with 100 µL of 2.98 mg/mL protease XIII solution in 1.0% formic acid at 0℃ and vortex-mixed for 2 minutes to prevent precipitation. The suspension was filtered with a 200 nm Supor filter, and frozen in liquid nitrogen

immediately. Then, 200 µL ice-cold acetonitrile was added to the frozen sample, which was directly infused into an LTQ-Orbitrap mass spectrometer at USF.

H/D Exchange mass spectrometry of protein on Ag nanoparticles

In solution: Aliquots of 10 µL of 160 pmol/µL myoglobin in 10 mM ammonium acetate buffer, pH 7.2, were each mixed with 90 µL of 10 mM ammonium acetate D_2O buffer, and incubated for different lengths of time to allow for H/D exchange (0, 1, 4, 15, and 60 minutes). The samples were digested with 100 µL of 2.98 mg/mL protease XIII (Aspergillus saitoi, Sigma) in 1.0% formic acid at 0℃ for 2 minutes. The solution was filtered through a 200 nm Supor filter, and immediately frozen in liquid nitrogen. Then 200 µL ice-cold acetonitrile was added to the frozen sample, which was directly infused into an LTQ-Orbitrap mass spectrometer at USF.

On Ag nanoparticles: A 100 µL aliquot of 16 pmol/µL myoglobin (0.272 mg/mL) in 10 mM ammonium acetate buffer, pH 7.2, was added to 5.44 mg of Ag nanoparticles (20-30 nm, QuantumSphere) and rotated for 5 hrs. The particle part was separated, washed, and a 10 µL suspension including most of the particles was mixed with 90 µL of 10 mM ammonium acetate D_2O buffer. The sample was incubated for different lengths of time to allow for H/D exchange (0, 1, 4, 15, and 60 minutes), digested with 100 µL of 2.98 mg/mL protease XIII solution in 1.0% formic acid at 0℃ and vortex-mixed for 2 minutes to prevent precipitation. The suspension was filtered with a 200 nm Supor filter, and immediately frozen in liquid nitrogen. Then 100 µL ice-cold acetonitrile was added to the frozen sample, which was directly infused into an LTQ-Orbitrap mass spectrometer at USF.

Results and Discussion

The peptide sequence mapping based on the results from the LTQ-Orbitrap is shown in Figure 4-9, together with previous mapping results from data obtained at the NHMFL for comparison. The spectra from Orbitrap data are very complex and hard to analyze in full scan mode, but many common fragments are observed when compared with the NHMFL data. The peptide coverages were almost the same in both cases, indicating that this procedure is a promising way to achieve the goals of this research.

The H/D exchange results (Figure 4-10) from the Orbitrap spectra show a mass shift during H/D exchange, even though in the solution samples, the mass increase is not very evident. However, all the residues showed a significant mass increase when adsorbed on silver nanoparticles. The mass increase can be better seen in Figure 4-11, which shows the deuterium atom uptake for residues 12-18, 39-48, and 32-42. During the H/D exchange, the general trend is that mass increases with the exchange time, but there are some fluctuations. More replicates are necessary to investigate this problem. Also, back exchange may be serious during the detection process. Care must be taken to address this issue. On the other hand, Figure 4-11 shows that there were significant mass increases from H/D exchange when myoglobin was adsorbed on nanoparticles. Deuterium uptake at 4 minutes for all the residues was much greater than that in solution, even after the exchange was performed in solution for more than 60 minutes. This preliminary result on the relative mass increases between the solution and on the nanoparticles is encouraging, since it clearly shows that upon adsorption on silver nanoparticles, significant conformational change occurred, resulting in greater deuterium uptake. It will be very interesting to investigate further how the myoglobin, or

other proteins on silver or other nanoparticles, change their global or local structure by the method developed here.

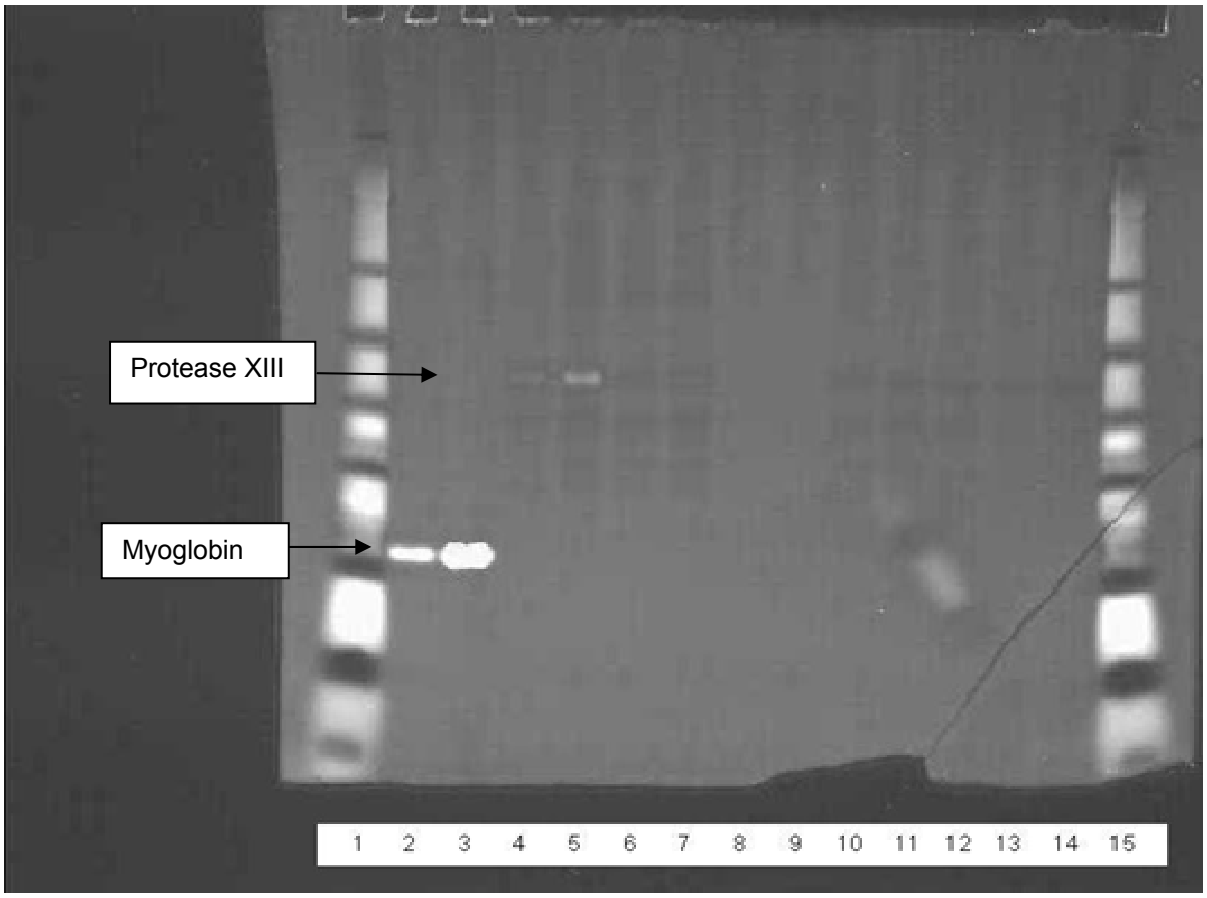

Figure 4-1. SDS-PAGE of freshly-made myoglobin digests and old samples. Samples 2,3 were prepared without filtration; others were prepared following filtration with 20 nm Alumina filter. 1) Blue plus 2 standard marker, 2) 5 μL myoglobin 80 pmol/μL + 45 μL Phosphate buffer + 50 μL 1% Formic acid, 3) 10 μl myoglobin 80 pmol/μL + 40 μL Phosphate buffer + 50 μL 1% Formic acid, 4) 50 μL protease XIII 1.4 mg/mL in 1% formic acid + 50 μL phosphate buffer, 5) 50 μL protease XIII 2.8 mg/mL in 1% formic acid + 50 μL phosphate buffer, 6)-14) digestion 2 minutes, 6) 5 μL myoglobin 80 pmol/μL + 45 μL phosphate buffer + 50 μL protease XIII 2.8 mg/mL in 1% formic acid, 7) 10 μL myoglobin 80 pmol/μL + 40 μL phosphate buffer + 50 μL protease XIII 2.8 mg/mL in 1% formic acid, 8)-10) & 12) 5 μL myoglobin 80 pmol/μL + 45 μL phosphate buffer + 50 μL protease XIII 1.4 mg/mL in 1% formic acid, 11) 10 μL myoglobin 80 pmol/μL + 40 μL phosphate buffer + 50 μL protease XIII 1.4 mg/mL in 1% formic acid, 13) sample to the NHMFL (5 μL myoglobin 80 pmol/μL + 45 μL D_2O phosphate buffer for one hour, then add 50 μL protease XIII 1.4 mg/mL in 1% formic acid), 14) sample to the NHMFL (5 μL myoglobin 80 pmol/μL + 45 μL phosphate buffer + 50 μL protease XIII 1.4 mg/mL in 1% formic acid), 15) Blue plus 2 standard marker

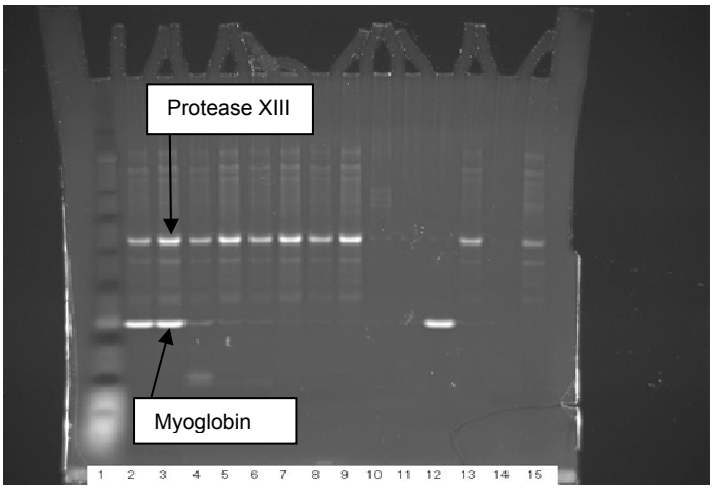

Figure 4-2. SDS-PAGE of freshly-made myoglobin digests. Samples 2-9, 12, 13 were prepared without filtration; others were prepared following filtration with 20 nm Alumina filter. 1) Blue plus 2 standard marker; 2) digestion 0 minute, final protease XIII 0.7mg/mL (5 μL myoglobin 80 pmol/μL + 45 μL phosphate buffer + 50 μL protease XIII 1.4 mg/mL in 1% formic acid); 3) digestion 0 minute, final protease XIII 1.4mg/mL (5 μL myoglobin 80 pmol/μL + 45 μL phosphate buffer + 50 μL protease XIII 2.8 mg/mL in 1% formic acid); 4) digestion 1 minute, final protease XIII 0.7mg/mL (5 μL myoglobin 80 pmol/μL + 45 μL phosphate buffer + 50 μL protease XIII 1.4 mg/mL in 1% formic acid); 5) digestion 1 minute, final protease XIII 1.4mg/mL (5 μL myoglobin 80 pmol/μL + 45 μL phosphate buffer + 50 μL protease XIII 2.8 mg/mL in 1% formic acid): 6) digestion 2 minutes, final protease XIII 0.7mg/mL (5 μL myoglobin 80 pmol/μL + 45 μL phosphate buffer + 50 μL protease XIII 1.4 mg/mL in 1% formic acid); 7) digestion 2 minutes, final protease XIII 1.4mg/mL (5 μL myoglobin 80 pmol/μL + 45 μL phosphate buffer + 50 μL protease XIII 2.8 mg/mL in 1% formic acid); 8) digestion 5 minutes, final protease XIII 0.7mg/mL (5 μL myoglobin 80 pmol/μL + 45 μL phosphate buffer + 50 μL protease XIII 1.4 mg/mL in 1% formic acid); 9) digestion 5 minutes, final protease XIII 1.4mg/mL (5 μL myoglobin 80 pmol/μL + 45 μL phosphate buffer + 50 μL protease XIII 2.8 mg/mL in 1% formic acid); 10) myoglobin blank after filtration (5 μL myoglobin 80 pmol/μL + 45 μL Phosphate buffer + 50 μL 1% formic acid); 11) protease XIII blank after filtration (50 μL protease XIII 1.4 mg/mL in 1% formic acid + 50 μL phosphate buffer); 12) myoglobin blank without filtration (5 μL myoglobin 80 pmol/μL + 45 μL Phosphate buffer + 50 μL 1% formic acid); 13) protease XIII without filtration (50 μL protease XIII 1.4 mg/mL in 1% formic acid + 50 μL phosphate buffer); 14) digestion 2 minutes, final protease XIII 0.7mg/mL, after filtration (5 μL myoglobin 80 pmol/μL + 45 μL phosphate buffer + 50 μL protease XIII 1.4 mg/mL in 1% formic acid); 15) digestion 2 minutes, final protease XIII 1.4mg/mL, after filtration (5 μL myoglobin 80 pmol/μL + 45 μL phosphate buffer + 50 μL protease XIII 2.8 mg/mL in 1% formic acid).

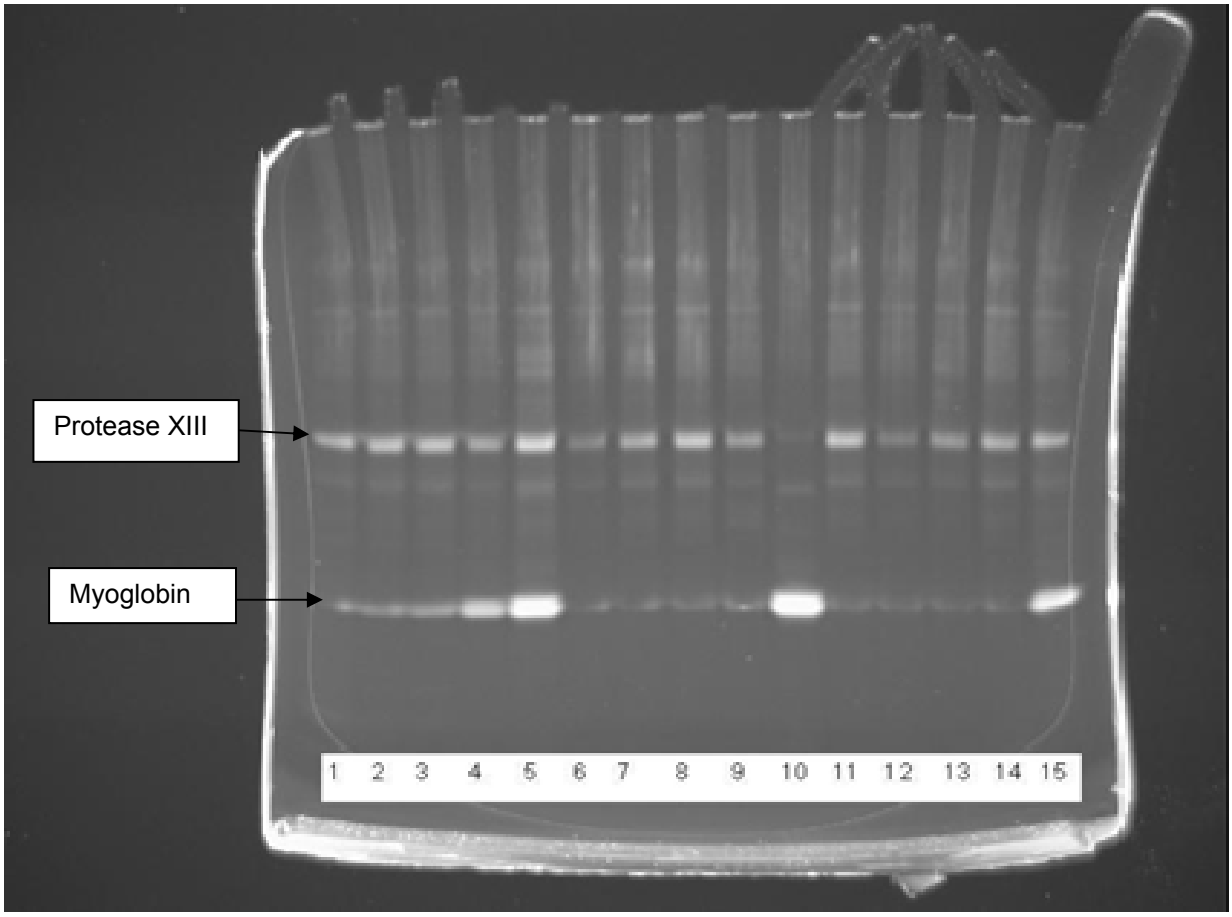

Figure 4-3. SDS-PAGE of freshly-made myoglobin digests. Samples 4-14 were prepared following filtration with 200 nm nylon filter. 1) digestion 2 minutes, final protease XIII 0.7mg/mL, myoglobin 0.07mg/mL, without filtration; 2) digestion 2 minutes, final protease XIII 1.4mg/mL, myoglobin 0.07mg/mL, without filtration; 3) digestion 2 minutes, final protease XIII 1.4mg/mL, myoglobin 0.14mg/mL, without filtration; 4) digestion 0 minute, final protease XIII 0.7mg/mL, myoglobin 0.07mg/mL; 5) digestion 0 minute, final protease XIII 1.4mg/mL, myoglobin 0.14mg/mL; 6) digestion 1 minute, final protease XIII 0.7mg/mL, myoglobin 0.07mg/mL; 7) digestion 1 minute, final protease XIII 1.4mg/mL, myoglobin 0.07mg/mL; 8) digestion 1 minute, final protease XIII 1.4mg/mL, myoglobin 0.14mg/mL; 9) digestion 2 minutes, final protease XIII 0.7mg/mL, myoglobin 0.07mg/mL; 10) myoglobin after filtration (10 μL myoglobin 80 pmol/μL + 40 μL Phosphate buffer); 11) digestion 2 minutes, final protease XIII 1.4mg/mL, myoglobin 0.14mg/mL; 12) digestion 5 minutes, final protease XIII 0.7mg/mL, myoglobin 0.07mg/mL; 13) digestion 5 minutes, final protease XIII 1.4mg/mL, myoglobin 0.07mg/mL; 14) digestion 5 minutes, final protease XIII 1.4mg/mL, myoglobin 0.14mg/mL; 15) digestion 0 minute, final protease XIII 0.7mg/mL, myoglobin 0.07mg/mL, without filtration.

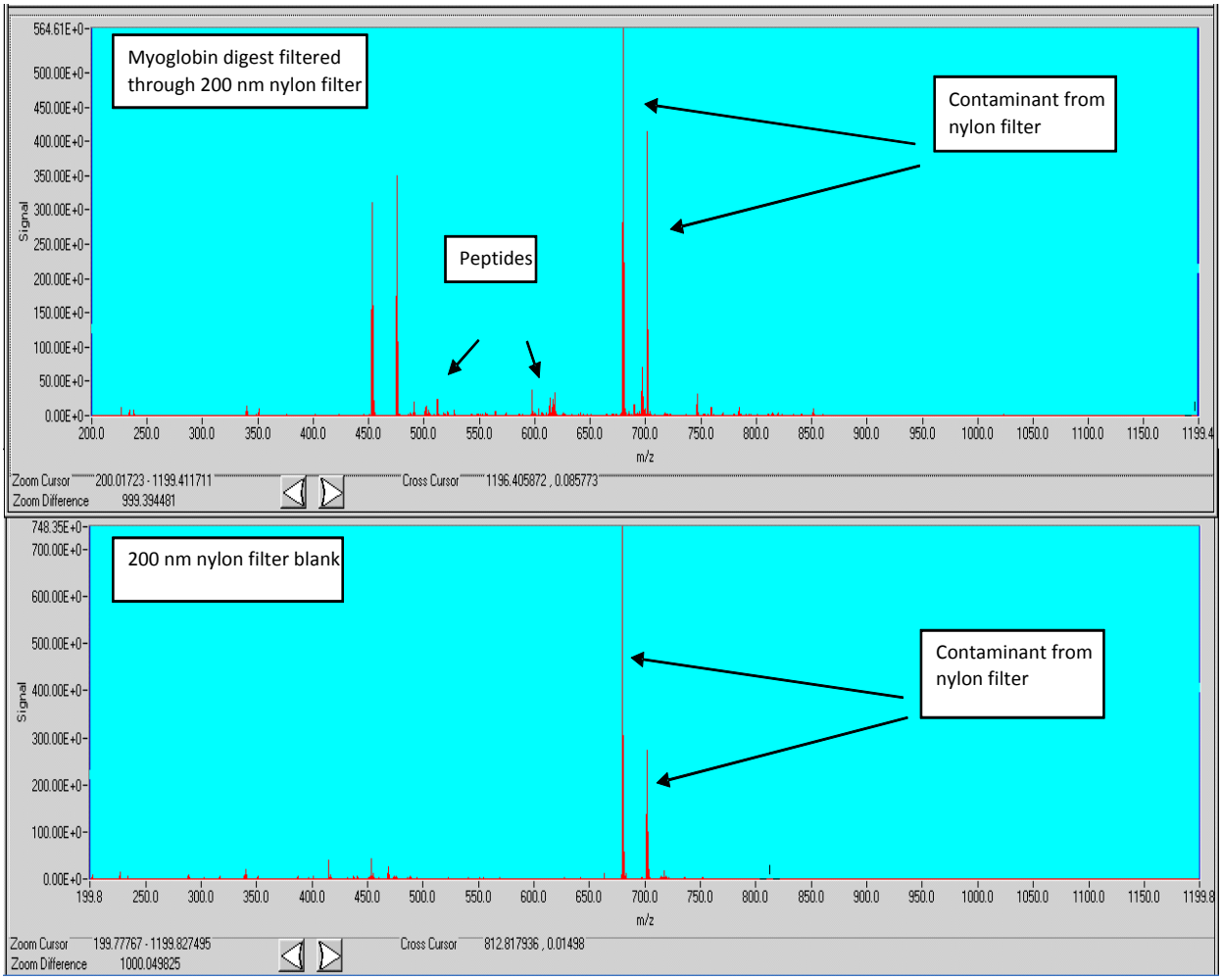

Figure 4-4. Mass spectra of myoglobin digests and blank following filtration with 200 nm nylon filter

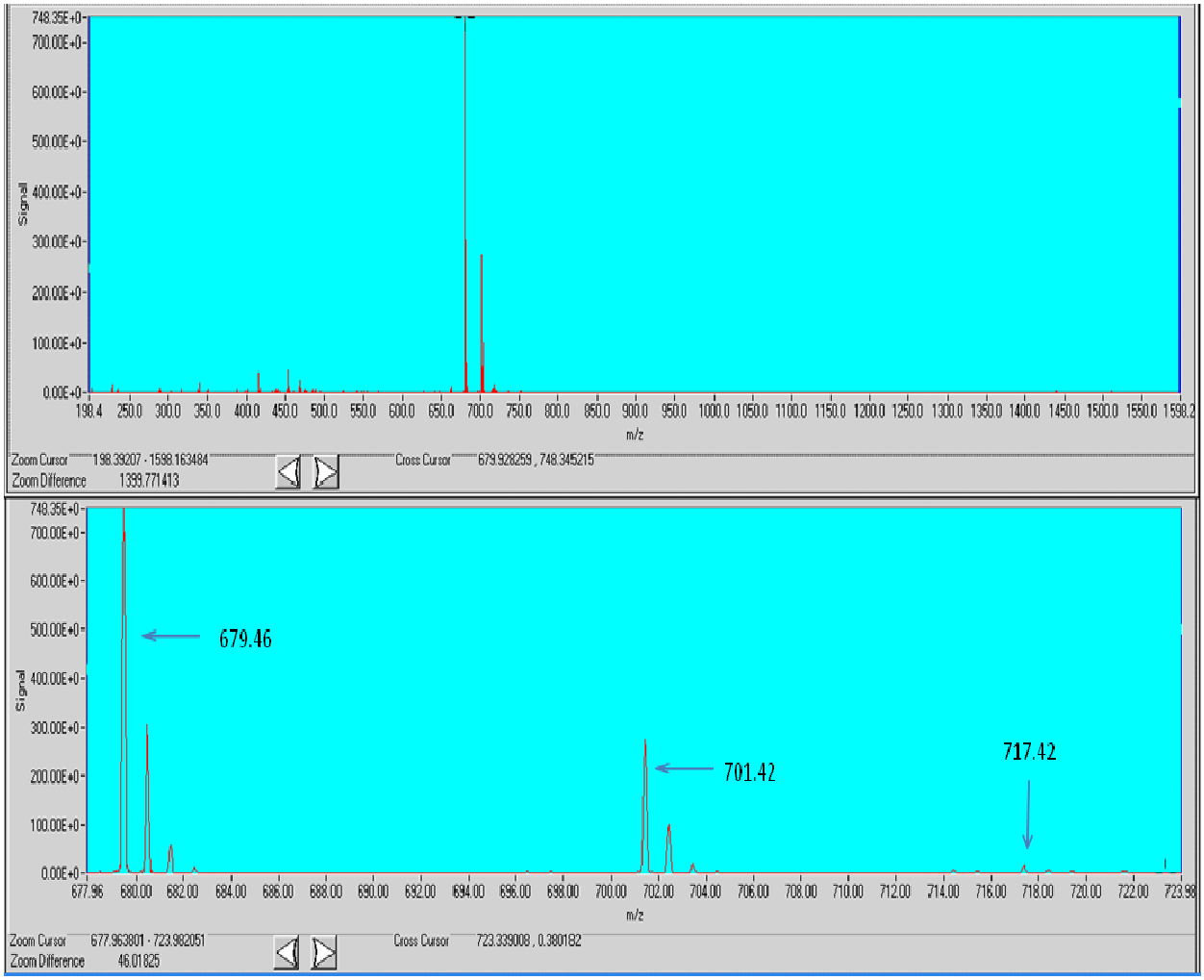

Figure 4-5. Mass spectrum of contaminants from 200 nm nylon filter

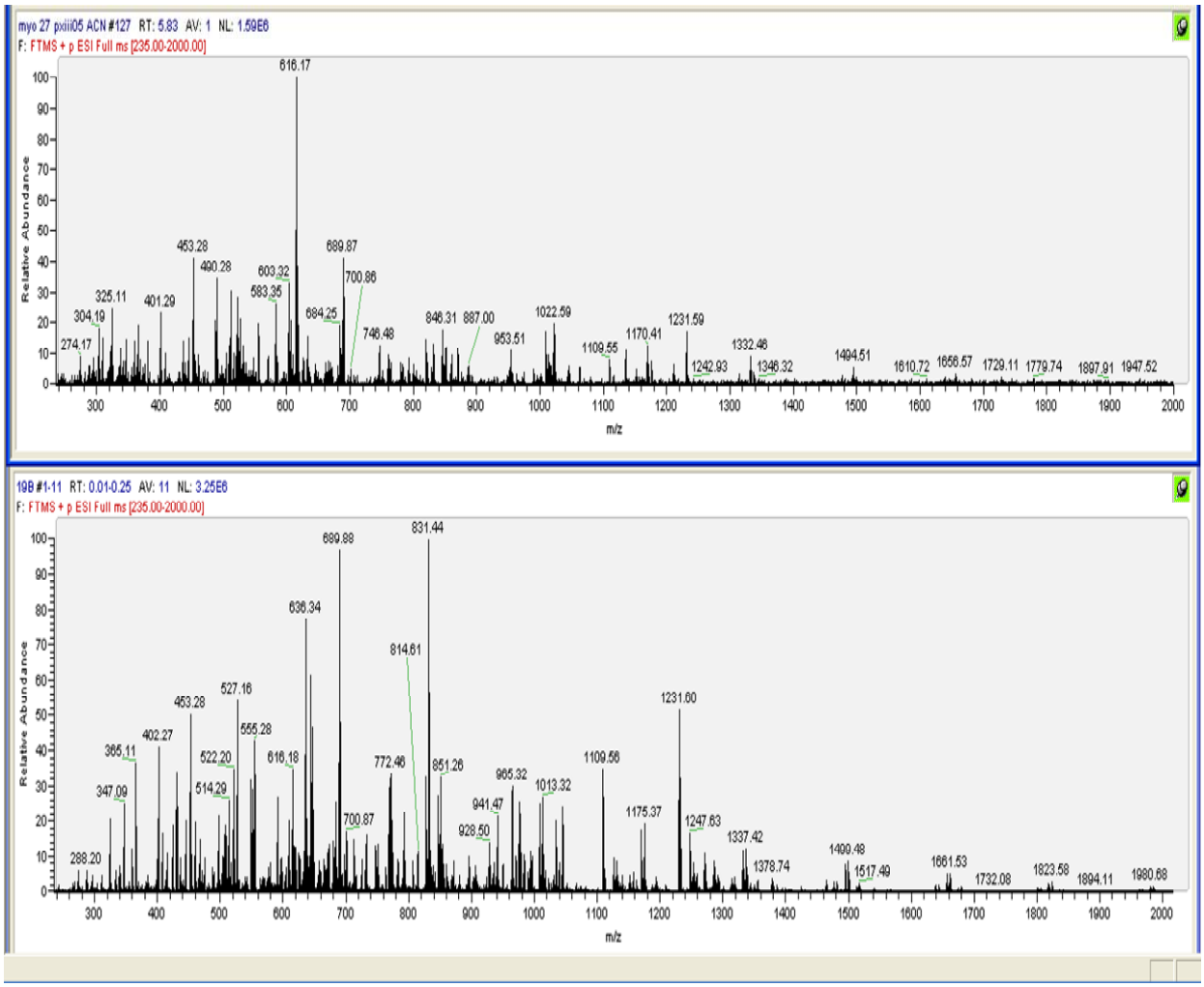

Figure 4-6. Mass spectrum of myoglobin digests following filtration with 200 nm Supor membrane

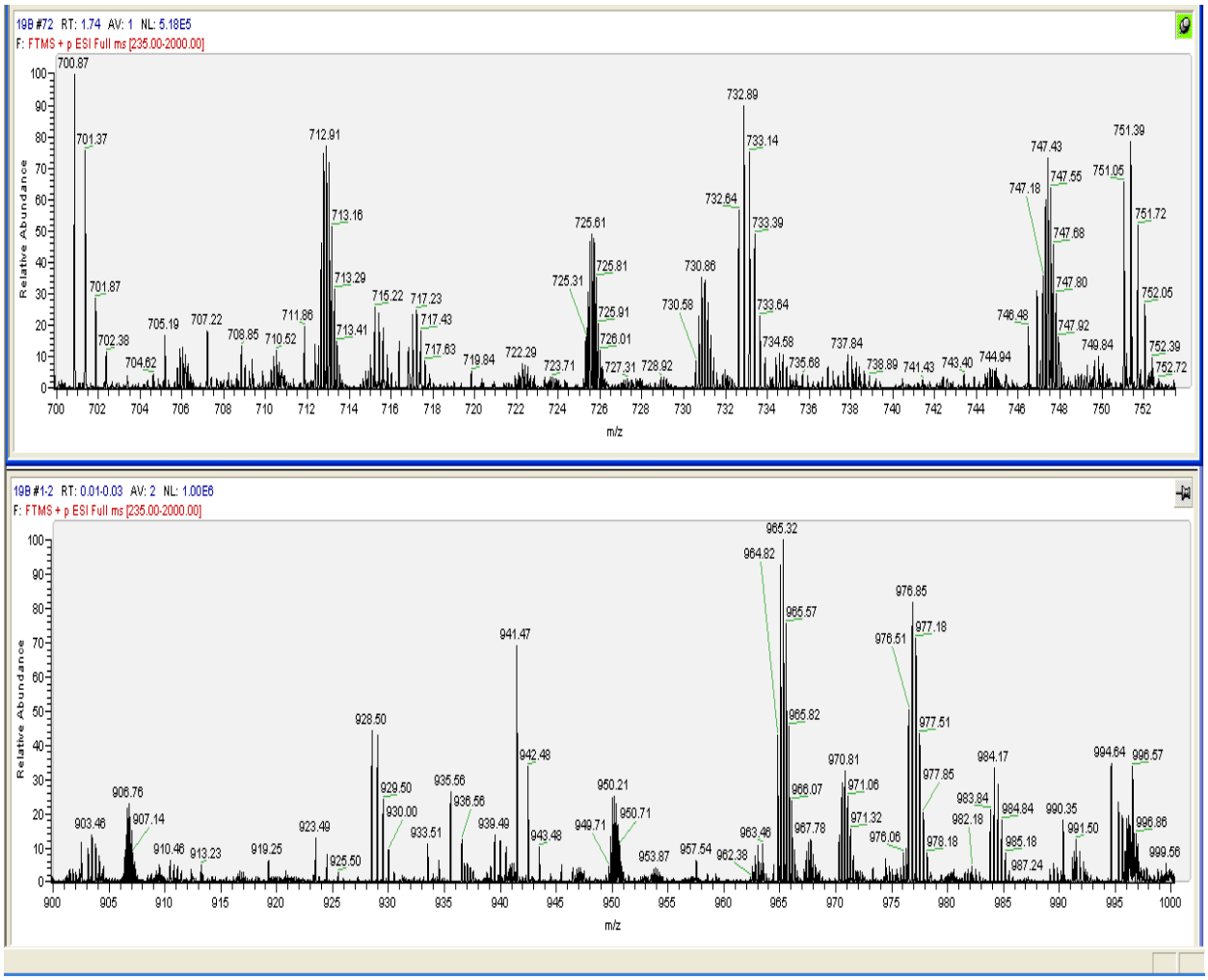

Figure 4-7. Zoomed-in mass spectra of myoglobin digests following filtration with 200 nm Supor membrane

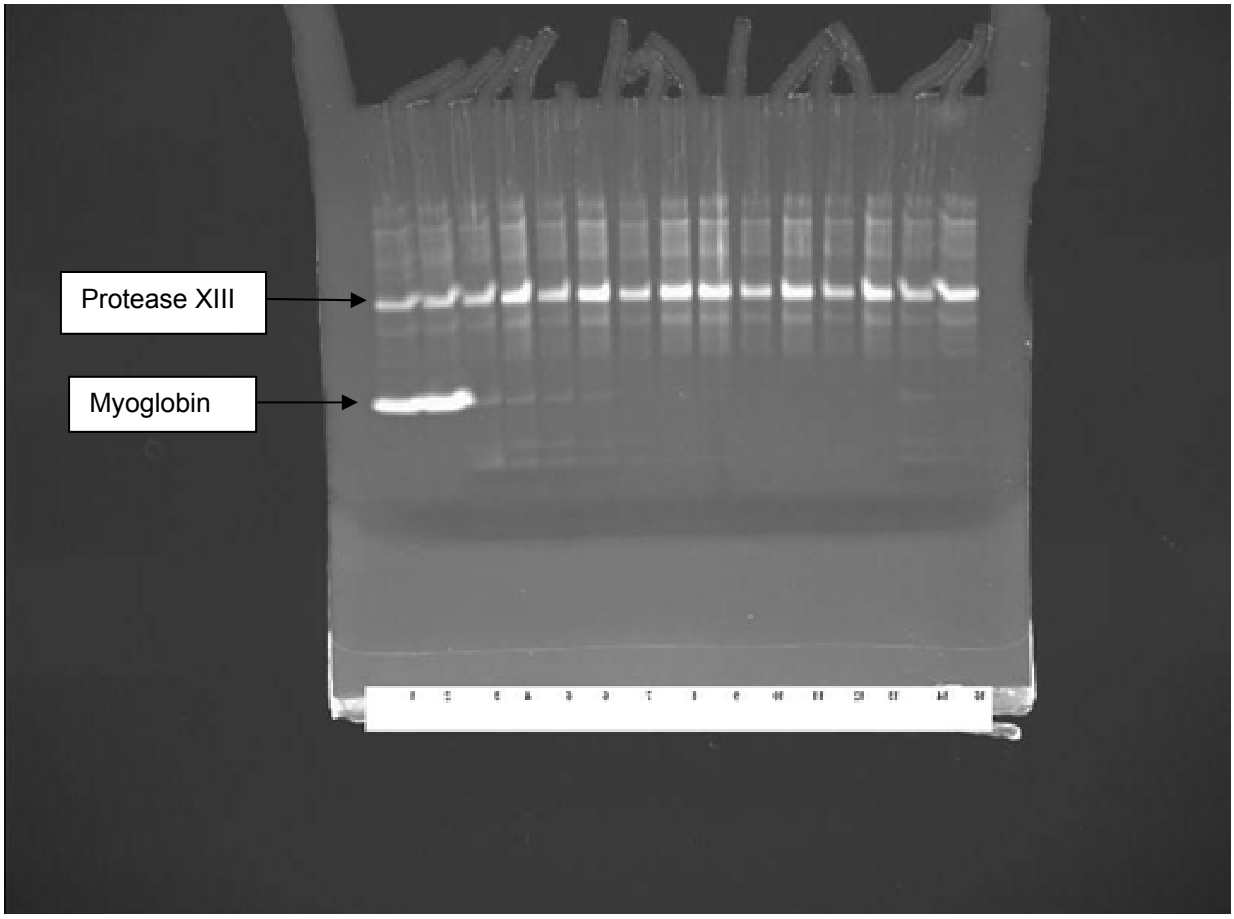

Figure 4-8. SDS-PAGE of myoglobin digested with protease XIII after 200 nm Supor membrane filtration. Samples 1-9 and14-15 are prepared without filtration, samples 10-13 are filtered with 200nm Supor filter. 1) digestion 0 minute, final protease XIII 0.7mg/mL, myoglobin 0.07mg/mL in low adhesion tube; 2) digestion 0 minute, final protease XIII 0.7mg/mL, myoglobin 0.07mg/mL in regular tube; 3) digestion 1 minute, final protease XIII 0.7mg/mL, myoglobin 0.07mg/mL; 4) digestion 1 minute, final protease XIII 1.4mg/mL, myoglobin 0.07mg/mL; 5) digestion 2 minutes, final protease XIII 0.7mg/mL, myoglobin 0.07mg/mL; 6) digestion 2 minutes, final protease XIII 1.4mg/mL, myoglobin 0.07mg/mL; 7) digestion 5 minutes, final protease XIII 0.7mg/mL, myoglobin 0.07mg/mL; 8) digestion 5 minutes, final protease XIII 1.4mg/mL, myoglobin 0.07mg/mL; 9) digestion 5 minutes, final protease XIII 1.4mg/mL, myoglobin 0.07mg/mL; 10) digestion 2 minutes, final protease XIII 0.7mg/mL, after filtration; 11) digestion 2 minutes, final protease XIII 1.4mg/mL, after filtration; 12) digestion 2 minutes, final protease XIII 0.7mg/mL, after filtration; 13) digestion 2 minutes, final protease XIII 1.4mg/mL, after filtration; 14) digestion 2 minutes, final protease XIII 0.7mg/mL, myoglobin 0.07mg/mL in regular tube; 15) digestion 2 minutes, final protease XIII 1.4mg/mL, myoglobin 0.07mg/mL in regular tube.

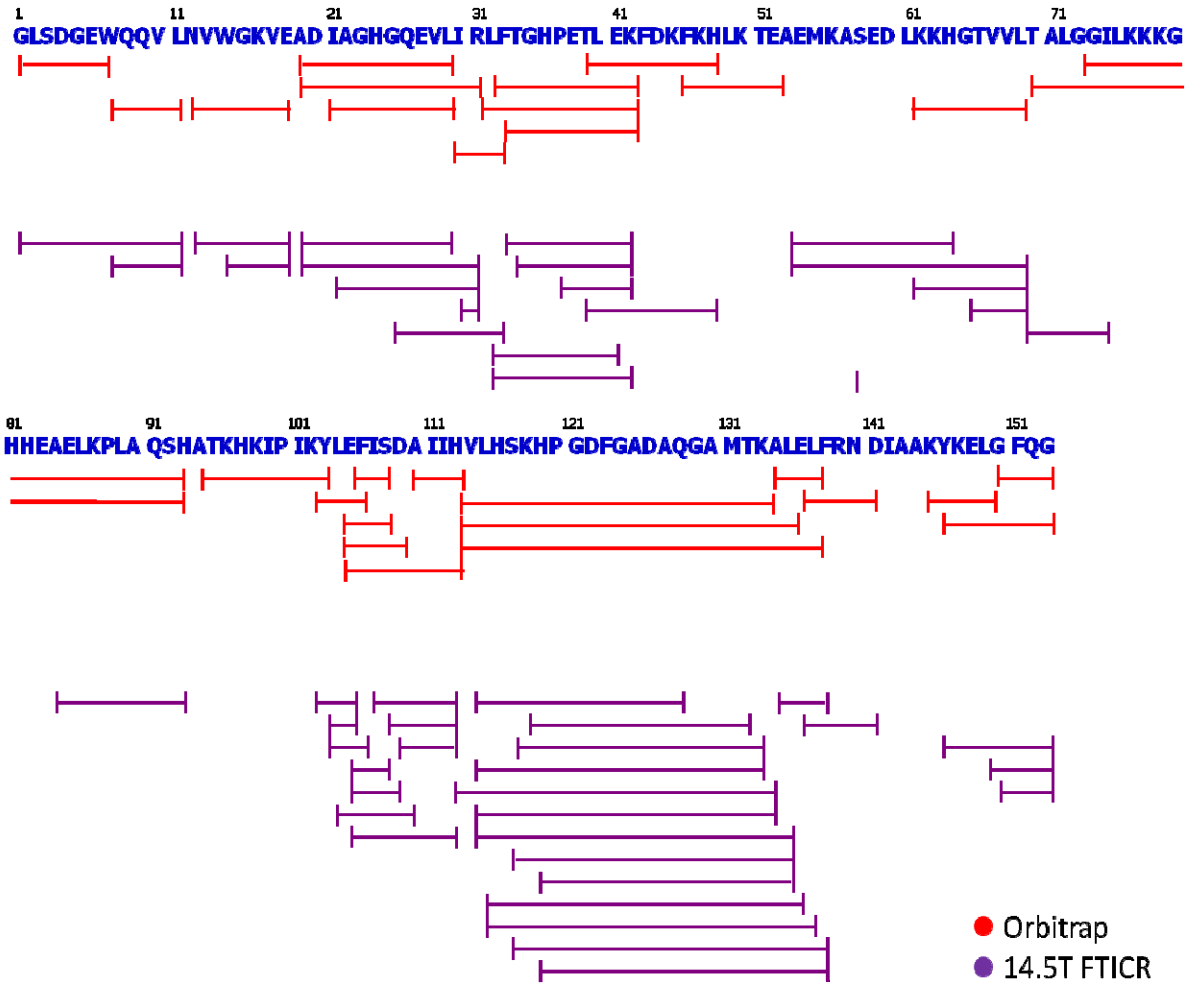

Figure 4-9. Peptide coverage of myoglobin digested with protease XIII

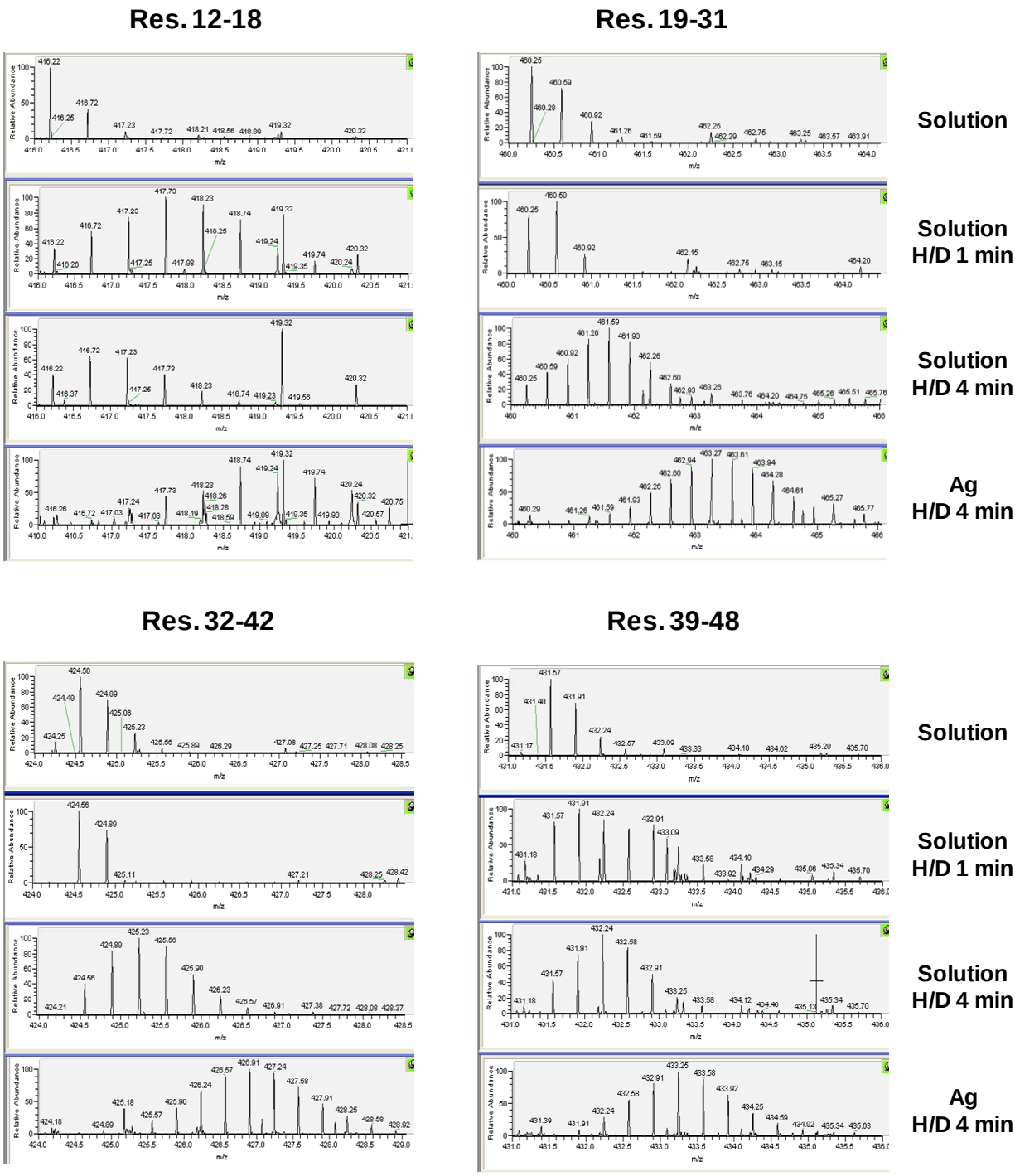

Figure 4-10. H/D exchange mass spectra of myoglobin in solution and on silver nanoparticles

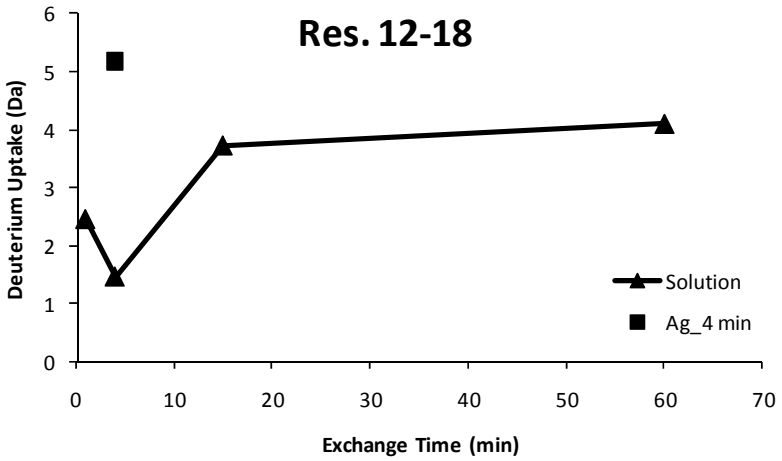

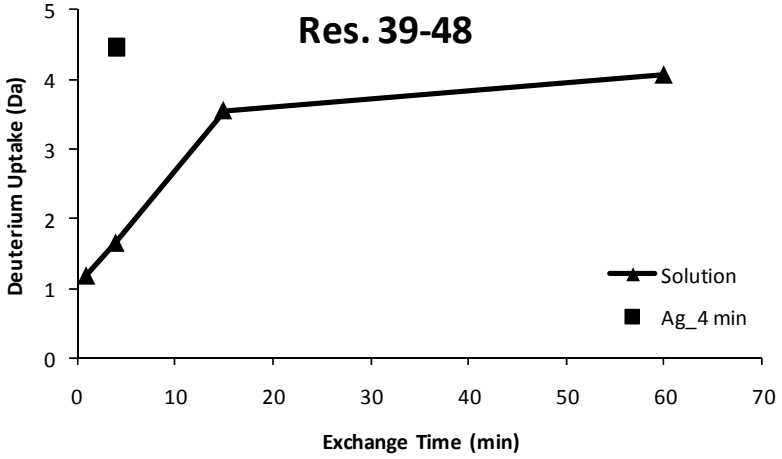

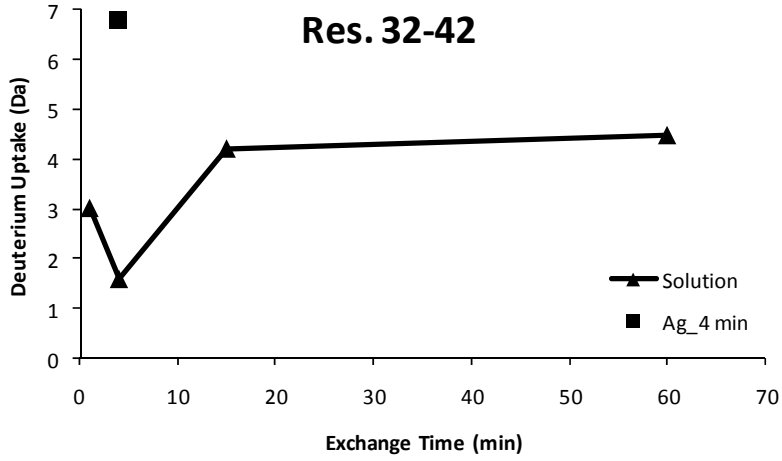

Figure 4-11. Deuterium uptake of myoglobin in solution and on silver nanoparticles

CHAPTER 5
CONCLUSIONS AND FUTURE WORK

Conclusions

This thesis explored the possibility of using hydrogen/deuterium exchange mass spectrometry in the study of conformational change of myoglobin in solution and adsorbed on nanoparticles. Adsorption experiments showed that the amounts of myoglobin adsorbed on different nanoparticles were significantly different, and were not directly related to the particle size within the range of this research. Pepsin and protease XIII were employed as the enzymes in digesting protein. Pepsin and protease XIII produced significantly different fragmentation patterns for myoglobin. Peptide fragments of myoglobin digested with protease XIII were smaller than those digested with pepsin. Both enzymes produced peptides which corresponded to protein coverage of over 85%. When comparing the peptide fragments coverage, it was found that the common peptide fragments (using protease XIII digestion) for myoglobin in solution and on silver nanoparticles cover about 75% of the protein chain, implying that the study of myoglobin conformational change on silver nanoparticles can be carried out using protease XIII and monitored with mass spectrometry. The peptide fragments for myoglobin in solution and on nanoparticles are somewhat different, indicating that the adsorption on nanoparticles can affect the protein fragmentation pattern, even if the same protease is used.

Filters can induce contamination during sample preparation and care must be taken to avoid contamination and to obtain strong mass spectrometric signals. Preliminary hydrogen/deuterium exchange results obtained using the Orbitrap mass spectrometer showed apparent differences in deuterium uptake between myoglobin in

solution and on silver nanoparticles, indicating that a conformational change occurred when myoglobin is adsorbed on nanoparticles.

Future Work

Hydrogen back exchange into the peptide backbone needs to be inhibited and monitored by using back exchange control and by optimizing the procedures in sample preparation, transportation, and analysis. In order to obtain a better picture of the conformation change of myoglobin on nanoparticles, more systematic experiments, including more replicates and more exchange times, are needed to elucidate the structural changes of myoglobin on nanoparticles in more detail.

During the sample preparation, HPLC may be used to check the efficacy of the sample preparation before real sample analysis using mass spectrometry. This will also eliminate the possibility of inducing contamination during sample preparation. Meanwhile, other characterization techniques, such as CD, fluorescence, DSC or NMR, may be used as complementary methods to confirm the credibility of the results.

LIST OF REFERENCES

(1) Auffan, M.; Rose, J.; Bottero, J.-Y.; Lowry, G. V.; Jolivet, J.-P.; Wiesner, M. R. *Nat Nano* **2009**, *4*, 634-641.

(2) Azad, N.; Rojanasakul, Y. *American Journal of Drug Delivery* **2006**, *4*, 79-88.

(3) Brayner, R. *Nano Today* **2008**, *3*, 48-55.

(4) Lynch, I.; Dawson, K. A. *Nano Today* **2008**, *3*, 40-47.

(5) Malmsten, M. In *Biopolymers at Interfaces,* 2nd ed.; Malmsten, M., Ed.; Marcel Dekker, Inc.: New York, USA, 2003, pp 711-740.

(6) Lynch, I.; Dawson, K. A.; Linse, S. *Sci. STKE* **2006**, *2006*, pe14-.

(7) Sabatino, P.; Casella, L.; Granata, A.; Iafisco, M.; Lesci, I. G.; Monzani, E.; Roveri, N. *Journal of Colloid and Interface Science* **2007**, *314*, 389-397.

(8) Norde, W.; Giacomelli, C. E. *Journal of Biotechnology* **2000**, *79*, 259-268.

(9) Couvreur, P.; Gref, R.; Andrieux, K.; Malvy, C. *Progress in Solid State Chemistry* **2006**, *34*, 231-235.

(10) Billsten, P.; Carlsson, U.; Elwing, H. In *Biopolymers at Interfaces,* 2nd ed.; Malmsten, M., Ed.; Marcel Dekker, Inc.: New York, USA, 2003, pp 497-515.

(11) van Mierlo, C. P. M.; Steensma, E. *Journal of Biotechnology* **2000**, *79*, 281-298.

(12) Arrington, C. B.; Robertson, A. D. In *Methods in Enzymology*; Academic Press, 2000; Vol. Volume 323, pp 104-124.

(13) Dempsey, C. E. *Progress in Nuclear Magnetic Resonance Spectroscopy* **2001**, *39*, 135-170.

(14) Tsutsui, Y.; Wintrode, P. L. *Current Medicinal Chemistry* **2007**, *14*, 2344-2358.

(15) Buijs, J.; Ramstrom, M.; Danfelter, M.; Larsericsdotter, H.; Hakansson, P.; Oscarsson, S. *Journal of Colloid and Interface Science* **2003**, *263*, 441-448.

(16) Klein, J. *Proceedings of the National Academy of Sciences* **2007**, *104*, 2029-2030.

(17) Cravello, L.; Lascoux, D.; Forest, E. *Rapid Communications in Mass Spectrometry* **2003**, *17*, 2387-2393.

(18) Zhang, H.-M.; Kazazic, S.; Schaub, T. M.; Tipton, J. D.; Emmett, M. R.; Marshall, A. G. *Analytical Chemistry* **2008**, *80*, 9034-9041.

(19) Allen, T. M.; Cullis, P. R. *Science* **2004**, *303*, 1818-1822.

(20) Lee, V. H. L. *Advanced Drug Delivery Reviews* **2004**, *56*, 1527-1528.

(21) FDA, 2008; Vol. 2009.

(22) Huang, Y.-H.; Zugates, G. T.; Peng, W.; Holtz, D.; Dunton, C.; Green, J. J.; Hossain, N.; Chernick, M. R.; Padera, R. F., Jr.; Langer, R.; Anderson, D. G.; Sawicki, J. A. *Cancer Res* **2009**, *69*, 6184-6191.

(23) Nel, A.; Xia, T.; Madler, L.; Li, N. *Science* **2006**, *311*, 622-627.

(24) Hlady, V.; Buijs, J. *Current Opinion in Biotechnology* **1996**, *7*, 72-77.

(25) Lundqvist, M.; Sethson, I.; Jonsson, B.-H. *Langmuir* **2004**, *20*, 10639-10647.

(26) Kelly, S. M.; Jess, T. J.; Price, N. C. *Biochimica et Biophysica Acta (BBA) - Proteins & Proteomics* **2005**, *1751*, 119-139.

(27) Chen, Y.; Barkley, M. D. *Biochemistry* **1998**, *37*, 9976-9982.

(28) Larsericsdotter, H.; Oscarsson, S.; Buijs, J. *Journal of Colloid and Interface Science* **2004**, *276*, 261-268.

(29) Larsericsdotter, H.; Oscarsson, S.; Buijs, J. *Journal of Colloid and Interface Science* **2005**, *289*, 26-35.

(30) Brandes, N.; Welzel, P. B.; Werner, C.; Kroh, L. W. *Journal of Colloid and Interface Science* **2006**, *299*, 56-69.

(31) Peng, Z. G.; Hidajat, K.; Uddin, M. S. *Colloids and Surfaces B: Biointerfaces* **2004**, *33*, 15-21.

(32) Woodward, C.; Simon, I.; Tuechsen, E. *Molecular and Cellular Biochemistry* **1982**, *48*, 135-160.

(33) Englander, S. W.; Kallenbach, N. *Quarterly Review of Biophysics* **1984**, *16*, 521-655.

(34) Hvidt, A.; Linderstrøm‐Lang, K. *Biochimica. Biophysica. Acta* **1954**, *14*, 574-575.

(35) Berger, A.; Linderstrom-Lang, K. *Archives of Biochemistry and Biophysics* **1957**, *69*, 106-118.

(36) Bai, Y.; Milne, J. S.; Mayne, L.; Englander, S. W. *Proteins: Structure, Function, and Genetics* **1993**, *17*, 75-86.

(37) Li, R.; Woodward, C. *Protein Science* **1999**, *8*, 1571-1590.

(38) Evans, J. N. S. *Biomolecular NMR Spectroscopy*; Oxford University Press: New York, USA., 1995.

(39) Bai, Y.; Englander, J. J.; Mayne, L.; Milne, J. S.; Englander, S. W.; Michael, L. J.; Ackers, G. K. In *Methods in Enzymology*; Academic Press, 1995; Vol. Volume 259, pp 344-356.

(40) Roder, H.; Norman, J. O.; James, T. L. In *Methods in Enzymology*; Academic Press, 1989; Vol. Volume 176, pp 446-473.

(41) Kaltashov, I. A.; Eyles, S. J. *Mass Spectrometry in Biophysics: Conformation and Dynamics of Biomolecules.*; John Wiley & Sons, Inc.: Hoboken, NJ, USA., 2005.

(42) Fenn, J. B.; Mann, M.; Meng, C. K.; Wong, S. F.; Whitehouse, C. M. *Science* **1989**, *246*, 64-71.

(43) Marshall, A. G.; Hendrickson, C. L. *International Journal of Mass Spectrometry* **2002**, *215*, 59-75.

(44) Makarov, A., Seattle, WA, May 28-June 8, 2006 2006.

(45) Richard, H. P.; Cooks, R. G.; Robert, J. N. *Mass Spectrometry Reviews* **2008**, *27*, 661-699.

(46) Baugh, J. A.; Donnelly, S. C. *J Endocrinol* **2003**, *179*, 15-23.

(47) Olmedo, D. G.; Tasat, D. R.; Guglielmotti, M. B.; Cabrini, R. L. *Journal of Biomedical Materials Research Part A* **2005**, *73A*, 142-149.

(48) Gilmanshin, R.; Dyer, R. B.; Callender, R. H. *Protein Science* **1997**, *6*, 2134-2142.

(49) Reymond, M. T.; Merutka, G.; Dyson, H. J.; Wright, P. E. *Protein Science* **1997**, *6*, 706-716.

(50) Langmuir, I. *Journal of the American Chemical Society* **1918**, *40*, 1361-1403.

(51) Griffitt, R. J.; Luo, J.; Gao, J.; Bonzongo, J.-C.; Barber, D. S. *Environmental Toxicology and Chemistry* **2008**, *27*, 1972-1978.

(52) Arai, T.; Norde, W. *Colloids and Surfaces* **1990**, *51*, 17-28.

(53) Senko, M. W.; Canterbury, J. D.; Guan, S.; Marshall, A. G. *Rapid Communications in Mass Spectrometry* **1996**, *10*, 1839-1844.

(54) Schaub, T. M.; Hendrickson, C. L.; Horning, S.; Quinn, J. P.; Senko, M. W.; Marshall, A. G. *Analytical Chemistry* **2008**, *80*, 3985-3990.

BIOGRAPHICAL SKETCH

Yaoling Long grew up living in Guilin, China, before she became an undergraduate student studying chemistry in Peking University, Beijing, China, where she obtained her Bachelor of Science and Master of Science degrees in chemistry. She started her graduate study in the Chemistry Department at the University of Florida in August 2006, supported by a financial aid from the graduate assistantship.